ENVIRONMENTAL EFFECTS ON STRESS CORROSION CRACKING OF TYPE 316L STAINLESS STEEL AND ALLOY 825 AS HIGH-LEVEL NUCLEAR WASTE CONTAINER MATERIALS

Prepared for

Nuclear Regulatory Commission
Contract NRC-02-93-005

Prepared by

Center for Nuclear Waste Regulatory Analyses
San Antonio, Texas

October 1994

Rec'd with letter dtd 4/5/94

CNWRA 94-028

ENVIRONMENTAL EFFECTS ON STRESS CORROSION CRACKING OF TYPE 316L STAINLESS STEEL AND ALLOY 825 AS HIGH-LEVEL NUCLEAR WASTE CONTAINER MATERIALS

Prepared for

Nuclear Regulatory Commission
Contract NRC-02-93-005

Prepared by

Gustavo A. Cragnolino
Darrell S. Dunn
Narasi Sridhar

Center for Nuclear Waste Regulatory Analyses
San Antonio, Texas

October 1994

426.1

PREVIOUS REPORTS IN SERIES

Number	Name	Date Issued
CNWRA 91-004	A Review of Localized Corrosion of High-Level Nuclear Waste Container Materials—I	April 1991
CNWRA 91-008	Hydrogen Absorption and Embrittlement of Candidate Container Materials	June 1991
CNWRA 92-021	A Review of Stress Corrosion Cracking of High-Level Nuclear Waste Container Materials—I	August 1992
CNWRA 93-003	Long-Term Stability of High-Level Nuclear Waste Container Materials: I—Thermal Stability of Alloy 825	February 1993
CNWRA 93-004	Experimental Investigations of Localized Corrosion of High-Level Waste Container Materials	February 1993
CNWRA 93-014	A Review of the Potential for Microbially Influenced Corrosion of High-Level Nuclear Waste Containers	June 1993
CNWRA 94-010	Review of Degradation Modes of Alternate Container Designs and Materials	April 1994

ABSTRACT

This report describes the experimental studies conducted to date in the Integrated Waste Package Experiments project to investigate the stress corrosion cracking of candidate container materials for the proposed high-level nuclear waste repository at Yucca Mountain. The effects of environmental variables, such as chloride concentration, the addition of thiosulfate, and temperature, on the stress corrosion cracking susceptibility of type 316L stainless steel and alloy 825 (Ni-29Fe-22Cr-3.0Mo-2.0Cu-1.0Ti) were studied in chloride-containing solutions with different cationic species (Mg^{2+}, Li^{+}, and Na^{+}) at temperatures ranging from 95 to 120 °C. Results of slow strain rate tests at both the open-circuit and anodically applied potentials were compared to those obtained under constant deflection conditions using U-bend specimens to determine the existence of a critical potential for stress corrosion cracking and the relationship of this potential to the repassivation potential for localized corrosion. It was confirmed that alloy 825 is significantly more resistant to stress corrosion cracking than type 316L stainless steel, using both constant deflection and slow strain rate tests, over a wide range of chloride concentrations. In constant deflection tests, type 316L stainless steel exhibited cracks above the vapor/solution interface in solutions containing 1,000 ppm chloride, indicating that the local environment created as a liquid film on the specimen surface could be more detrimental than the bulk environment.

CONTENTS

TABLES

FIGURES

FIGURES (cont'd)

ACKNOWLEDGMENTS

The author gratefully acknowledges the technical review of Fred F. Lyle, Jr. and the programmatic review of Wesley C. Patrick. Appreciation is due to Bonnie L. Garcia for her assistance in the preparation of this report.

This report was prepared to document work performed by the Center for Nuclear Waste Regulatory Analyses (CNWRA) for the Nuclear Regulatory Commission (NRC) under Contract No. NRC-02-93-005. The activities reported here were performed on behalf of the NRC Office of Nuclear Regulatory Research (RES), Division of Regulatory Applications. The report is an independent product of the CNWRA and does not necessarily reflect the views or regulatory position of the NRC. Sources of data are referenced in each section. CNWRA-generated laboratory data contained in this report meet quality assurance requirements described in the CNWRA Quality Assurance Manual. For all other data, their respective sources should be consulted for determining their level of quality assurance.

EXECUTIVE SUMMARY

The Nuclear Regulatory Commission (NRC) regulation 10 CFR 60.113 requires waste packages to provide substantially complete containment of radionuclides for a minimum period of 300 to 1,000 years. As a result of this requirement, two key technical uncertainties (KTUs), identified by the NRC during the development of the License Application Review Plan, are addressed in the Integrated Waste Package Experiments (IWPE) program. These uncertainties are the extrapolation of short-term laboratory and prototype test results to predict long-term performance of waste packages, and the prediction of environmental effects on the performance of the packages. The resolution of these technical uncertainties is addressed in the IWPE project through five interconnected tasks: Task 1—Corrosion; Task 2—Stress Corrosion Cracking; Task 3—Materials Stability; Task 4—Microbiologically Influenced Corrosion; Task 5—Other Degradation Modes, using a suitable combination of literature surveys and experimental results.

The present report is part of the activities conducted under Task 2, which is focused on the experimental studies conducted on stress corrosion cracking (SCC) of two candidate container materials. These materials belong to the class of the austenitic Fe-Ni-Cr-Mo alloys and have been tentatively selected by the U.S. Department of Energy (DOE) for the proposed repository site at Yucca Mountain. These materials, type 316L stainless steel (SS) and alloy 825, were among those initially selected as candidate alloys for the single-wall container design of the waste package presented in the Site Characterization Plan. Type 316L SS is currently being proposed as the material of choice for the multi-purpose canister (MPC), whereas alloy 825 is being considered for the inner disposal overpack in the multiple engineered barrier approach for the waste package recently adopted by DOE.

SCC is one of the most important potential modes of degradation of the candidate materials proposed for use as containers in the geological disposal of high-level nuclear waste. In addition, it is a phenomenon difficult to predict as a result of the synergistic coupling of material, environmental, and mechanical factors. Slow strain rate tests and constant deflection tests on mill-annealed type 316L SS and alloy 825 are being used to define environmental conditions, in terms of solution composition, pH, and temperature, as well as potential ranges that may promote SCC. The environments of interest are chloride-containing solutions that simulate variations of groundwater environments produced by evaporation of water and concentration of salts. The ultimate goal is to determine if a critical potential for SCC exists, and then define the relationship between this potential and the repassivation potential for pitting/crevice corrosion. If such critical potential for SCC exists, it can be used as a bounding parameter for the prediction of long-term behavior, assuming that various combinations of tensile stress conditions in the container can promote cracking under the range of environments anticipated at the repository site.

The experimental results provided in this report are consistent with the assumption that the repassivation potential for localized corrosion constitutes a lower bound for the critical potential for SCC in the case of type 316L SS. However, the occurrence of SCC is apparently dependent on test technique. In slow strain rate tests, SCC of type 316L SS was promoted by concentrated chloride solutions (>7.2 molal Cl^-) above 100 °C, and at lower chloride concentrations in the presence of thiosulfate. In contrast, no SCC was observed with this technique at chloride concentrations lower than 5.8 molal, even in the presence of thiosulfate. On the other hand, SCC was observed on type 316L SS, but not in alloy 825, using U-bend specimens in constant deflection tests conducted in more dilute solutions containing thiosulfate. It was noted that the susceptibility to localized corrosion and cracking is more pronounced in areas of the specimens in which a liquid film is formed on their surfaces above the vapor/solution

interface, suggesting that the local environment created in this location is more detrimental than the bulk environment.

As expected, alloy 825 was found to be far more resistant to SCC than type 316L SS, failing in slow strain rate tests only in solutions containing 14 molal Cl^- at 120 °C. The constant deflection tests confirmed the results of the slow strain rate tests in the case of alloy 825 in the sense that no SCC was found within the same range of chloride concentrations using both test methods. Contrary to the case of type 316L SS in which a significant susceptibility to SCC in constant deflection tests was detected in the vapor phase, under conditions leading to the formation of liquid film on the surface, localized corrosion in the form of pitting was the predominant phenomenon in alloy 825.

The approach adopted in the study of SCC considering the repassivation potential for localized corrosion as the critical potential for the occurrence of SCC needs further confirmation through additional testing. Based on the results and analyses of tests described in this report, a series of experiments is recommended including crack arrest experiments, long-term experiments lasting from a few months to 5 yr, tests using fracture mechanics specimens, and an integrated localized corrosion/SCC test including heat transfer effects and the influence of periodic wet-dry cycles. The need to extend SCC studies to the materials proposed for the outer disposal overpack in the current DOE design of the waste package is indicated.

1 INTRODUCTION

The Nuclear Regulatory Commission (NRC) regulation 10 CFR 60.113 requires waste packages to provide substantially complete containment of radionuclides for a minimum period of 300 to 1,000 years. Arising from this requirement is the need for the U.S. Department of Energy (DOE) to demonstrate, through proper selection, design, testing, and analyses, the long-term performance of waste packages. In order to evaluate the DOE resolution of these technical issues, NRC must develop an understanding of the important factors that affect long-term performance of waste package materials and components. Other considerations are the suitability and limitations of various test methods used to demonstrate performance, as well as the influence of factors not addressed by the DOE that may affect the performance of waste packages. The Integrated Waste Package Experiments (IWPE) program at the Center for Nuclear Waste Regulatory Analyses (CNWRA) supports the NRC in attaining these objectives. The overall technical objectives of the IWPE Project are to:

- Develop a good understanding of the information currently available on metal corrosion and on other metal-degradation processes
- Assess waste package materials and designs selected by the DOE and provide independent evaluation for reasonable assurance of long-term performance
- Conduct waste package experiments to scope and study the key parameters affecting long-term material performance
- Support the Office of Nuclear Regulatory Research (RES) in addressing the needs of the Division of Waste Management (DWM)

Two key technical uncertainties (KTU), developed as part of the compliance determination strategy (CDS) and listed in the License Application Review Plan (LARP), Sections 5.2 and 5.4 (Nuclear Regulatory Commission, 1992), are addressed in the IWPE program. These uncertainties are:

- The extrapolation of short-term laboratory and prototype test results to predict long-term performance of waste packages and engineered barrier systems (EBS)
- The prediction of environmental effects on the performance of waste packages and the EBS

The resolution of these technical uncertainties are addressed in the IWPE project through five interconnected tasks:

Task 1—Corrosion
Task 2—Stress Corrosion Cracking
Task 3—Materials Stability
Task 4—Microbiologically Influenced Corrosion
Task 5—Other Degradation Modes

The present report is part of the activities conducted under Task 2, which is focused on the experimental studies conducted on stress corrosion cracking (SCC) of two candidate container materials belonging to

the class of the austenitic Fe-Ni-Cr-Mo alloys. These alloys are among those tentatively selected by the DOE for the proposed repository site at Yucca Mountain.

In the U.S. geologic disposal program, the conceptual design of the waste package proposed by the DOE has changed from a thin-walled container of a corrosion-resistant alloy, emplaced in a partially lined, vertical borehole and surrounded by an air gap (U.S. Department of Energy, 1988), to a more robust design that is still evolving. The design being developed in the Advanced Conceptual Design phase of the Waste Package Plan is based on the use of multiple engineered barriers to achieve the required containment of the waste form. In a recently proposed design (U.S. Department of Energy, 1993a), a large number of spent fuel assemblies [(e.g., 12/21 pressurized water reactor (PWR) or 24/40 boiling water reactor (BWR) assemblies)] will be arranged inside a thin-walled container, termed a multi-purpose canister (MPC), as a permanent component of the waste package during transportation, storage, and disposal. In addition to the MPC, outer casks of varying materials and designs will be used for transportation and storage. For disposal, the waste package will be composed of an inner containment barrier immediately surrounding the MPC, and an outer containment barrier (U.S. Department of Energy, 1993b). These barriers are usually designated as inner and outer disposal overpacks. These large, multibarrier waste packages will be emplaced horizontally in drifts, probably surrounded by crushed tuff as backfill material (Ruffner et al., 1993). However, several aspects of the conceptual and detailed designs of the waste package are still evolving. Additional information presented by DOE was reviewed in a recently published report (Sridhar et al., 1994), in which the literature on the SCC of possible disposal overpack materials was critically examined. Previously, all the relevant literature on the SCC of corrosion-resistant alloys selected as candidate materials for the thin-wall container concept was also reviewed (Cragnolino and Sridhar, 1992).

It has been proposed that high thermal loading be used to create a dry-out zone around the Engineered Barrier System (EBS) for thousands of years that will minimize corrosion and nongaseous radionuclide transport (Buschek et al., 1993). The drying out process may create deposition of solids rich in Ca and Si and solutions rich in Na and K (Beavers et al., 1992; Murphy and Pabalan, 1994). However, backflow of the condensate through fractures intersecting the borehole may result in an aqueous environment around the container, as indicated by the results of some field heater tests (Patrick, 1986; Zimmerman et al., 1986; Ramirez, 1991). The evaporation of water and the rewetting of the dried solids may cause the formation of solutions rich in chloride and sulfate, as derived through modeling by Walton (1993) and shown experimentally by Abraham et al. (1986) and Beavers et al. (1992). Hence, a conservative approach to life prediction is to assume the presence of aqueous conditions surrounding the containers, at least episodically. This assumption is conservative because the corrosion rate in a dry steam or dry air environment at anticipated repository temperatures is negligible (Farmer et al., 1991). The chemical composition of such an aqueous environment is not known, and a range of concentrations of various species should be explored. A detailed explanation of the reasons for the expected changes in the composition and properties of the environment surrounding the waste packages as a consequence of radioactive decay heat and radiolysis has been provided (Sridhar et al., 1993a; 1993b).

For evaluating "substantially complete containment" in the example analysis of a reference container (Cragnolino et al., 1994), it was assumed that corrosion failure modes of importance to life prediction are determined by the corrosion potential. The corrosion potential of the container material, which is a mixed potential dictated by the kinetics of the anodic and cathodic reactions at the surface exposed to the repository environment, changes with time in response to factors such as radiolysis, pH, temperature, and oxygen concentration (Macdonald and Urquidi-Macdonald, 1990). If the corrosion potential exceeds the

pit-initiation potential (E_p), pits initiate and propagate into the container wall. If the corrosion potential drops below E_p but remains above the repassivation potential (E_{rp}), pits already initiated continue to grow, but no new pits initiate. Finally, if the corrosion potential drops below E_{rp}, all pits repassivate and cease to grow. After repassivation, the corrosion of the container continues in a uniform manner at a low rate determined by the passive current density. This concept of critical potentials has been well established in the literature for pitting and crevice corrosion (Szklarska-Smialowska, 1986).

Given the uncertainties in the type of waste package design that will be used by DOE and in the composition of the environment that will be encountered by the waste packages, it is important to establish, where possible, experimental methodologies that will apply to classes of materials rather than particular alloys and to investigate the effects of environmental factors over wide ranges. Furthermore, it is important to demonstrate that these experimental techniques can be used to derive long-term performance functions of the waste package materials. Both aspects, as they apply to the phenomena of SCC, are addressed in this report.

SCC is one of the potential modes of degradation of the candidate materials proposed for use as containers in the geological disposal of high-level nuclear waste (HLW) (Cragnolino and Sridhar, 1992). SCC is defined as a phenomenon by which ductile metals and alloys fail in a brittle manner through the initiation and propagation of cracks resulting from the combined action of a sustained tensile stress (applied and/or residual) and a specific corrosive environment. This phenomenon is one of the most insidious forms of metal failure because it usually occurs in metal and alloys that are extremely resistant to uniform corrosion as a result of the formation of a film on the metal surface that slows down the corrosion rate. These films may be passivating layers, tarnish films, or dealloyed layers. The concept of critical potential has been applied to SCC of many alloy-environment combinations (Cragnolino and Sridhar, 1992), but there are no data for the alloys and environments of interest to the Yucca Mountain repository.

Indeed, both type 316L stainless steel (SS) and alloy 825 are considered primary candidate materials for the MPC (Sridhar et al., 1994), and experimental studies on the effects of environmental factors and potential on the SCC of these two materials are the main focus of this report. Slow strain rate and constant deflection tests were used to define environmental conditions, in terms of solution composition, pH, and temperature, as well as potential ranges that promote SCC. The environments studied are mainly chloride-containing solutions that simulate variations of groundwater environments produced by evaporation of water and concentration of salts. The ultimate goal is to determine if a critical potential for SCC exists, and to define then the relationship between this potential and the repassivation potential for pitting/crevice corrosion. If such critical potential for SCC exists, it can be used as a bounding parameter for the prediction of long-term behavior assuming that various combinations of tensile stress conditions in the container would be sufficiently high to induce cracking under the range of environmental conditions anticipated at the repository site.

Initial tests were conducted on type 316L SS to evaluate the validity of the slow strain rate technique for this type of studies. It is known (Cragnolino and Sridhar, 1992) that this alloy is susceptible to SCC in relatively dilute chloride-containing solutions at temperatures above 80 °C, as demonstrated by many failures under service conditions in a wide range of industrial applications. However, contradictory results have been obtained in the application of this technique to nonsensitized austenitic SSs, suggesting that tests may have been conducted at strain rates that are too high to detect SCC or at open-circuit potentials located outside the cracking susceptibility range (Beavers and Koch, 1992). Another possibility is that the

stressing conditions found in practical applications cannot be easily reproduced in slow strain rate tests or the test duration is not long enough for crack initiation to occur. The effect of test technique on SCC was, therefore, investigated, and the slow strain rate tests were complemented with SCC tests under constant deflection conditions using U-specimens under both open-circuit and potentiostatic controlled conditions.

2 EXPERIMENTAL

The chemical compositions of the heats of type 316L SS and alloy 825 used in this study are given in Table 2-1. The heats of both materials designated as A were obtained in the form of hot-rolled and annealed plates, 12.7 mm (0.5 in.) thick, and used for slow strain rate tests. Detailed characterization of these two heats was reported previously (Sridhar et al., 1993a). No grain boundary precipitation was observed, but MnS inclusions were detected in type 316L SS and cuboidal particles of Ti (C,N) in alloy 825. Round specimens were machined with the tensile axis perpendicular to the rolling direction from bars cut from the plates, after the bars were centerless ground to a diameter of 6.35 mm (0.245 in.). Two types of specimens were used. One of them was a round, smooth tensile specimen with a waisted section having a gage length of 12.7 mm (0.5 in.) and a diameter of 3.175 mm (0.125 in.). The other type was a round, notched specimen, in which a circumferential notch, with a depth of 1.588 mm (0.0625 in.), an included angle of 60°, and a radius of 51 μm, was machined. The notched specimen was used to facilitate crack initiation. In some tests, an O-ring was placed in the notch position to create an artificial crevice. Except when noted, tests were conducted with the alloys in the as-received condition, without any heat treatment after machining. The specimens were wet-ground longitudinally along the gage length with 600-grit SiC paper, and washed with acetone and deionized water just before the tests.

Table 2-1. Chemical compositions of the heats of type 316L stainless steel and alloy 825 used in this study

Alloy/Heat	Elemental Composition, wt percent										
	Al	C	Cr	Cu	Fe	Mn	Mo	Ni	P	S	Others
316L SS/A	NA	0.014	16.35	0.27	Bal.	1.58	2.07	10.04	0.026	0.018	Si:0.49 N:0.06
316L SS/B	NA	0.019	16.30	NA	Bal.	1.90	2.13	10.18	0.030	0.001	Si:0.50 N:0.03
825/A	0.07	0.016	22.09	1.79	30.41	0.35	3.21	41.06	0.028	0.023	Si:0.19 Ti:0.82
825/B	0.09	0.010	22.07	1.72	29.69	0.40	3.49	41.22	NA	0.001	Si:0.29 Ti:1.02

The heats of type 316L SS and alloy 825 designated as B in Table 2-1 were used for the preparation of specimens for constant-deflection tests. These heats were obtained in the form of cold-rolled and mill-annealed sheets, 3.175 mm (0.125 in.) thick. U-bend specimens were machined from these sheets and stressed, without any heat treatment, to a radius of bend curvature of 6.35 mm (0.25 in.), using an appropriate device according to American Society for Testing and Materials (ASTM) Practice G 30-90 (American Society for Testing and Materials, 1991). Bolts and nuts made of alloy C-276, electrically isolated from the specimens by zirconia spacers, were used for the single-stage stressing operation. The resulting tensile stress was perpendicular to the rolling direction (transverse specimens), and the total strain on the outer fiber of the bend was estimated to be about 25.0 percent, using the expression given in ASTM Practice G 30-90. After bending, the specimens were cleaned in 10-percent HNO_3 at room

temperature for 1 hr to remove any accidental surface contamination with steel particles produced during the bending operations. The specimens were then rinsed in deionized water.

2.1 SLOW STRAIN RATE TESTS

The slow strain tests were conducted according to an international standard (International Organization for Standardization, 1989) using machines in which the pull rods holding the specimens were electrically isolated from the frame. Solutions (approximately 350 mL in volume) were contained in electrochemical cells made of glass and polytetrafluoroethylene (PTFE). The temperature was maintained at the desired value by using external heating tapes, a platinum resistance temperature detector (RTD), and a temperature controller. The cells were fitted with a gas bubbler and a water-cooled condenser connected to a water trap to prevent evaporation of water and back-diffusion of air. A platinum electrode and a saturated calomel electrode (SCE) were used as counter and reference electrodes, respectively. A Luggin capillary with a porous silica tip connected the cell, through a salt bridge containing a cotton wick, to the SCE, which was located in a separate reservoir at room temperature. Accordingly, all the potentials are referred to the SCE scale at ambient temperature (22 °C), without correction for the thermal diffusion potential along the nonisothermal salt bridge.

Most of the tests were conducted under potentiostatic conditions. Potentials were controlled using an Electrosynthesis Model 440 multichannel potentiostat, connected through a Strawberry Tree ACPC-16-16, 16-bit, 16-channel analog-digital converter (ADC) and an ACAO 12-8, 12-bit, 8-channel digital/analog converter (DAC) to an Austin 386 computer. In addition to the potential and the current, measured as a potential drop through a 10-ohm resistor, voltage signals from load cells and linear voltage differential transducers (LVDT) were also fed into the ADC through appropriate signal conditioners. The load cells and the LVDT were used to measure the load on the specimen and its extension, respectively, during the course of the test. The data acquisition was performed using the Workbench® software. This software is an icon-based program through which external instruments are controlled, signals are acquired, and algebraic and logical operations can be performed in order to obtain the required data in the appropriate units. The data were then stored on a magnetic disk for further analysis. In addition, the potential and the current were checked independently by using a electrometer and a picoammeter, respectively. The load cells and the LVDTs, in conjunction with their corresponding signal conditioners, were calibrated using a proving ring and a micrometer, respectively, as standards.

In the initial set of slow strain rate tests, the solutions contained 85 ppm HCO_3^-, 10 ppm NO_3^- and 2 ppm F^-, with the addition of 1,000 or 10,000 ppm Cl^- and 20, 1,000 or 10,000 ppm SO_4^{2-}. All these anions were added as Na^+ salts. The solutions were prepared with reagent grade chemicals and double deionized water. Solution compositions were selected on the basis of the localized corrosion studies previously reported, in which E_p, E_{rp}, and E_{corr} values for type 316L SS and alloy 825 were determined (Sridhar et al., 1993a). All these tests were conducted at 95 °C under potentiostatic conditions, and the solutions were purged either with N_2 gas to remove the dissolved oxygen, or with CO_2 to attain a pH close to 5.0, simultaneously removing oxygen. A single test was conducted under open-circuit conditions. In this case, synthetic air (79%N_2–21%O_2) was bubbled into the solution. In some tests, the pH of the solutions was initially adjusted to pH 4.0 by the addition of HCl.

A second set of tests was conducted in the same solutions as above with the addition of 0.001 or 0.01 mol/L of $Na_2S_2O_3$. These tests were performed at 95 °C, and the solutions were purged with CO_2. A third set of slow strain rate tests was performed in concentrated chloride solutions, prepared with

salts of different cations (Mg^{2+}, Li^{+}, and Na^{+}) but without the presence of additional anions. The solutions in this set of tests were fully deaerated with nitrogen. Additional tests were conducted in concentrated NaCl solutions with the addition of thiosulfate to compare the behavior of alloy 825 with that of type 316L SS. In these tests, the solutions were purged with CO_2 and the temperature was 95 °C. Several tests were performed using a specially designed crevice-forming device, made of perfluoroalkoxy (PFA) tubing and a PTFE holder, mounted in the gage length of the smooth tensile specimens. These tests were conducted either under potentiostatic or galvanostatic control in 1 molar NaCl solution, acidified to pH 4.0, to determine if cracks can be initiated under occluded cell conditions leading to active crevice corrosion.

An extension rate of 1.27×10^{-5} mm/s (5.0×10^{-7} in./s), which represents an initial strain rate of 1.0×10^{-6} s^{-1} for the smooth tensile specimens, was used in the first series of slow strain rate tests. For the notched specimens, this nominal extension rate may represent a strain rate at the notch tip at least two orders of magnitude greater than that for the smooth specimens. The extension rate was reduced to 4.6×10^{-6} mm/s (1.8×10^{-7} in./s) and to 2.8×10^{-6} mm/s (1.1×10^{-7} in./s) in several tests to increase the sensitivity of the slow strain rate technique.

After a specimen was mounted inside the cell, the solution was purged with the selected gas and then heated to the desired temperature. The specimen was allowed to attain a steady-state corrosion potential before the selected potential was applied. In tests conducted under galvanostatic conditions, a constant current was applied, and the corrosion potential was monitored during the course of the test. An initial load of approximately 133 N (30 lb) was applied to the specimen, and straining was started as soon as a steady current or potential was obtained. After failure, the fracture and side surfaces of all specimens tested were examined with a stereoscope. Selected specimens were further examined in the scanning electron microscope (SEM). Such examination was conducted after corrosion products deposited in the fracture and side surfaces were ultrasonically removed using a solution of 3 mL of concentrated HCl in 50 mL of double deionized water, inhibited with 4 mL of 2-butyne-1,4 diol (35-percent aqueous solution).

2.2 CONSTANT DEFLECTION TESTS

Constant deflection tests were conducted simultaneously in four 1-L glass cells using the experimental setup described previously (Sridhar and Cragnolino, 1993; Sridhar et al., 1993a). Two U-bend specimens were tested simultaneously in each cell. Except when noted, the specimens were partially immersed in the solutions such that the legs of the U-bend were in the vapor space while the apex of the bend was completely submerged in the liquid. One of the specimens was exposed to the solution at a controlled anodic potential, whereas the second one was maintained under open-circuit conditions. The multichannel potentiostat and the remaining electronic instrumentation for controlling the potential and for data acquisition were similar to that described above for the slow strain rate tests.

The constant deflection tests were performed in most of the solutions used for slow strain rate tests. Solutions containing 1,000 ppm chloride with and without the addition of $Na_2S_2O_3$ were used in some tests. Concentrated chloride solutions prepared with either LiCl or NaCl reagents were used to compare the effect of both cations on the SCC behavior of both type 316L SS and alloy 825. These solutions were prepared using double-deionized water with the pH adjusted to 4.0. In some tests, $Na_2S_2O_3$ was added to concentrated chloride solutions to compare the results with those from the slow strain rate tests. The constant deflection tests were conducted initially for a period of 21 to 22 d. Later tests were conducted in successive periods of 28 d. At the end of each period, the specimens were

optically examined at a magnification of about 70× after being cleaned using a ultrasonic cleaner. If no signs of SCC or severe localized corrosion were detected, the same specimens were exposed, using freshly prepared solutions, to identical environments for an additional time interval. In all these tests, the temperature of the solutions was maintained at 95 °C. Selected specimens were examined in the SEM, and then cross-sectioned and mounted for metallographic observation of cracks.

3 RESULTS

3.1 SLOW STRAIN RATE TESTS

3.1.1 Type 316L Stainless Steel

As noted previously, one of the main objectives of these tests was to demonstrate a possible relationship between the repassivation potential for pitting/crevice corrosion and a critical potential for SCC that defines the lower limit of the susceptibility range. To select the appropriate potentials for slow strain rate testing of type 316L SS, E_p, E_{rp}, and E_{corr} obtained at 95 °C on unstressed specimens, using a scan rate of 0.167 mV/s (Sridhar et al., 1993a), were plotted as a function of chloride concentration, as shown in Figure 3-1. Following an abrupt decrease at low chloride concentrations, both E_p and E_{rp} decrease linearly with the logarithm of chloride concentration at concentrations above 100 ppm. These two potentials define a potential range that contracts from approximately 400 mV at 100 ppm Cl^- to 200 mV at 10^5 ppm Cl^-. This potential range is that within which SCC could be expected (Cragnolino and Sridhar, 1992), because pitting corrosion should predominate at higher potentials, whereas at lower potentials any tendency to crack initiation would be overcome by the repassivation of the locally damaged passive film. It is also seen in Figure 3-1 that E_{corr} is practically independent of the chloride concentration with values slightly lower than -600 mV_{SCE}, indicating that the predominant cathodic reaction is the reduction of hydrogen ions because oxygen has been removed from the solution. As shown in Table 3-1, potentials located between E_{rp} and E_p were selected for slow strain rate testing in a variety of solutions in which the chloride concentration was changed from 1,000 to 10,000 ppm and the sulfate concentration decreased from 10,000 to 20 ppm. The initial pH of these solutions was modified from 8.1 to 4.0 or 5.4, either by the addition of HCl or by bubbling CO_2.

The results of the first set of slow strain rate tests are detailed in Table 3-1 and summarized in Figure 3-2. It is seen that no SCC was observed in any of these tests, even at relatively high potentials within the potential range defined by E_{rp} and E_p. The elongation to failure was found to be 55.6 percent on average for all the smooth tensile specimens exhibiting ductile failure with a standard deviation of approximately 10 percent, indicating a high degree of ductility but a relatively large dispersion in the elongation values. In a single case, a specimen failed as a result of severe pitting corrosion, exhibiting an elongation of only 20.2 percent. This failure occurred at the highest potential tested in the solution of pH 4.0 containing 10,000 ppm Cl^- and 10,000 ppm SO_4^{2-}, even though this potential (0 mV_{SCE}) was lower than the corresponding E_p. In other tests, predominantly ductile failure accompanied by pitting corrosion was observed leading to a reduced elongation to failure as compared to the cases in which purely ductile failure occurred. It can be concluded from these results that pitting is initiated at potentials lower than E_p in prolonged tests, but pits do not seem to act as initiation sites for cracks under these experimental conditions.

All these tests were conducted potentiostatically, with the exception of one test carried out under open-circuit conditions in which synthetic air (79 vol% N_2—21 vol% O_2) was bubbled into the solution. The corrosion potential decreased during the test from 0 to -200 mV_{SCE}, but only ductile failure was observed. As shown in Table 3-1, E_{corr} varied from -330 to -250 mV_{SCE} in most of the tests, as measured before straining was initiated. These values are about 300 mV higher than those plotted in Figure 3-1, corresponding to solutions deaerated by bubbling N_2. The difference can be attributed to the

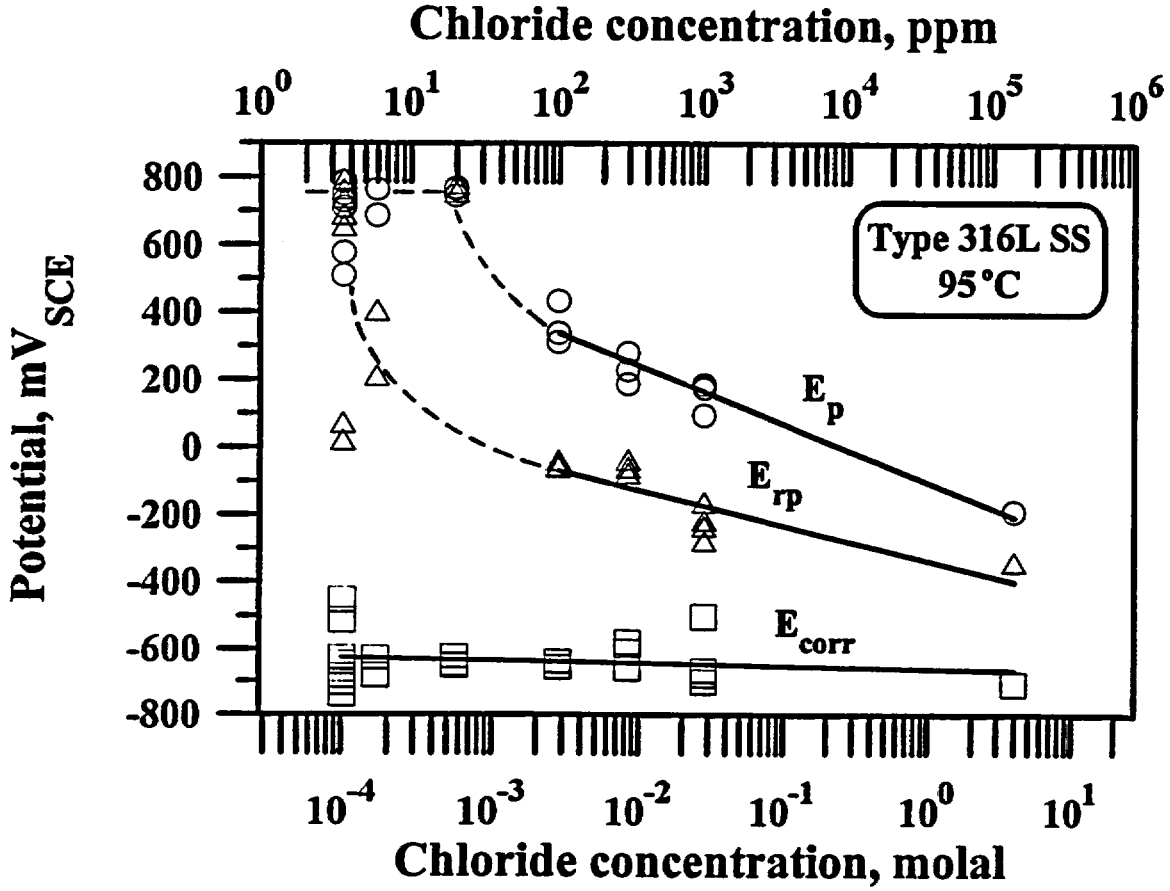

Figure 3-1. Effect of chloride concentration on pitting (E_p), repassivation (E_{rp}), and corrosion (E_{corr}) potentials of type 316L stainless steel in simulated groundwater (pH 8.1 to 8.4) at 95 °C, measured on unstressed specimens using a scan rate of 0.167 mV/s

lower pH attained by purging the solutions with CO_2, which leads to the higher value of the corrosion potential in these dilute chloride solutions.

No SCC was observed, even in some specific tests in which a piece of PTFE tape was wrapped around the gage section of tensile specimens in order to promote crevice conditions that may lead to crack initiation. The use of notched specimens did not lead to the initiation of cracks, although an O-ring was used to create crevice conditions. It was expected that a notch would facilitate crack initiation by localized intensification of the stress, avoiding the simultaneous initiation at several cracks. However, it appears that the extension rate at the root of the notch was too high, and ductile failure occurred before any crack could be initiated. It should be noted that the failure times for tests conducted with notched specimens were shorter than those for tensile specimens, by a factor of about four, which significantly decreases the exposure time. It appears that the extension rate should be reduced, at least by an order of magnitude, to promote crack initiation in a notched specimen.

Table 3-1. Results of slow strain rate tests ($\dot{\varepsilon}=1\times10^{-6}\ s^{-1}$) of type 316L stainless steel in dilute chloride solutions at 95 °C

Spec.	Cl^- (ppm)	SO_4^{2-} (ppm)	Gas	E_{corr} (mV_{SCE})	E_{app} (mV_{SCE})	Current (A)	Initial pH	Final pH	Elong. (%)	Failure Time (h)	Test Results
S	10,000	10,000	N_2	—	0	10^{-2}	4.0	—	20.2	59.5	Severe pitting
S	10,000	10,000	Air	0 to −200	O.C.	—	4.0	—	57.8	167.9	Ductile failure
S	1,000	1,000	N_2	—	0	10^{-5} to 10^{-6}	7.0	—	61.0	221.0	Ductile failure
S	1,000	20	CO_2	−510	50 to 0	3×10^{-4} to -6×10^{-6}	—	5.3	68.0	196.0	Ductile failure
S	1,000	20	CO_2	−520	100	1×10^{-4} to 8×10^{-4}	—	5.4	46.2	131.5	Ductile failure/ pitting
S	10,000	20	CO_2	−260	−100	-3×10^{-5} to 2×10^{-4}	—	5.3	55.0	152.0	Ductile failure
S	10,000	20	CO_2	−260	−50	10^{-4} to 10^{-3}	—	5.5	43.8	89.4	Ductile failure/ pitting
S	10,000	20	CO_2	−310	−50	2.0×10^{-4}	—	6.4	41.4	135.6	Ductile failure/ pitting
S[a]	10,000	20	CO_2	−320	−100	5×10^{-4} to 3×10^{-3}	—	5.4	57.8	162.9	Ductile failure/ pitting
S[a]	10,000	20	CO_2	−330	−130	5×10^{-6} to 1×10^{-5}	—	5.6	68.6	88.9	Ductile failure
N	1,000	20	CO_2	−250	100	5.0×10^{-3}	—	5.5	2.41[c]	58.9	Ductile failure
N[b]	1,000	20	CO_2	−260	0 to −280	5.2×10^{-6}	—	—	1.52[c]	57.5	Ductile failure
N[b]	1,000	20	CO_2	—	50	5.3×10^{-5}	—	—	1.78[c]	48.9	Ductile failure
N[b]	1,000	20	CO_2	−250	80	-5×10^{-6} to 10^{-3}	8.1	5.2	2.11[c]	45.5	Ductile failure
N[b]	10,000	20	CO_2	−250	−100	-1×10^{-5} to 5×10^{-4}	7.8	5.6	2.18[c]	47.3	Ductile failure

S – Smooth specimen N – Notched specimen O.C. – Open circuit a – with PTFE tape b – with O-ring c – extension in mm

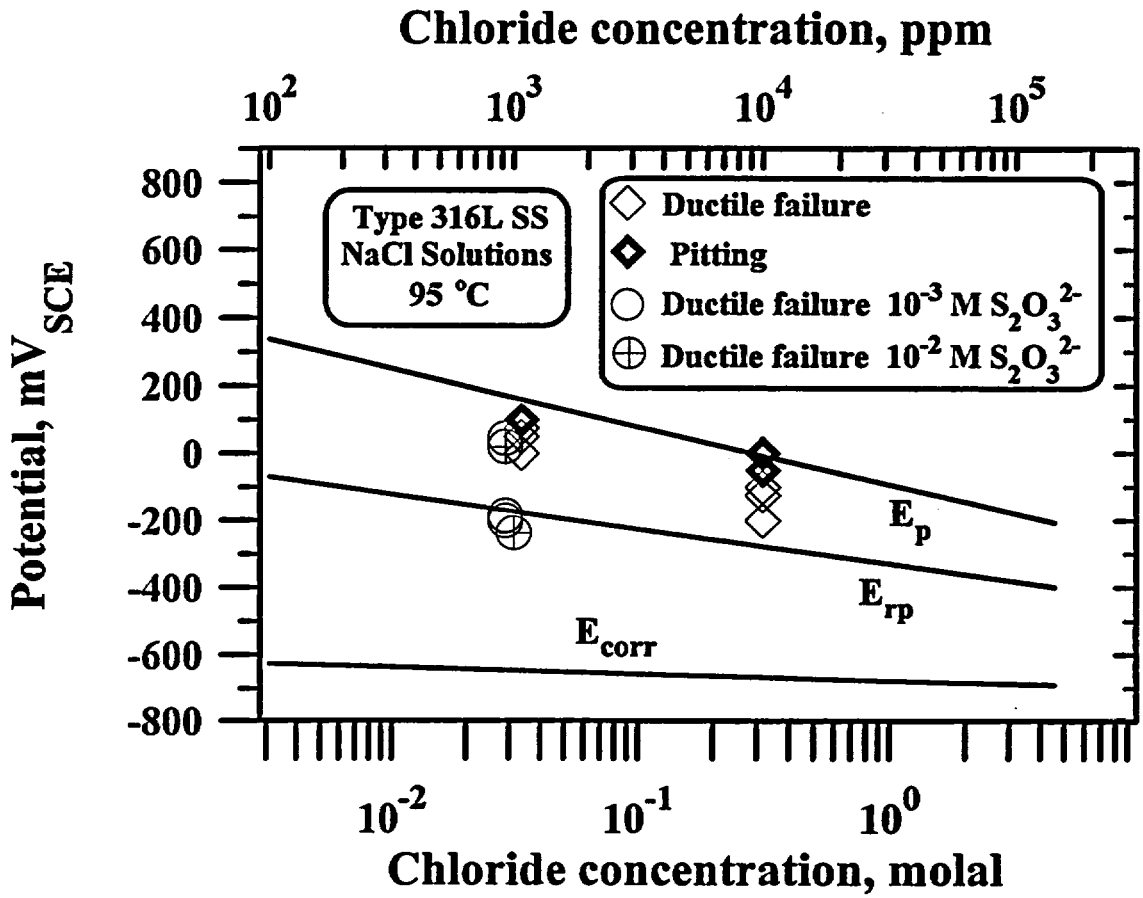

Figure 3-2. Potentials and chloride concentrations selected for slow strain rate tests of type 316L stainless steel in dilute chloride solutions at 95 °C with and without the addition of thiosulfate, in relation to pitting (E_p) and repassivation (E_{rp}) potentials

Slow strain rate tests were conducted in solutions containing 1,000 ppm chloride with the addition of thiosulfate, based on the suggestion of Lott and Alkire (1989) that thiosulfate can be generated by the dissolution of MnS inclusions present in certain austenitic SSs, such as type 304 and 316. In addition, thiosulfate is an anionic species of interest because it can be formed as a byproduct of the metabolism of sulfate-reducing bacteria (Geesey, 1993). In conjunction with chloride, thiosulfate promotes passivity breakdown in these alloys. It is known that transgranular cracking of quench-annealed austenitic SSs in chloride solutions initiates from localized corrosion trenches or slots where breakdown of the passive films occurs (Silcock and Swann, 1979). Concentrations of thiosulfate equal to 0.001 and 0.01 mol/L were chosen because Newman et al. (1982) reported the most significant decrease in the pitting potential of type 304 SS in chloride-containing solutions by the addition of thiosulfate within that range of concentrations. Potentials were selected to avoid widely distributed pitting corrosion and then adjusted during the course of the test to avoid significant increases in current associated with pit initiation.

As shown in Table 3-2, no SCC was observed in the presence of either 0.001 or 0.01 mol/L of $Na_2S_2O_3$, even at an applied potential 280 mV above the open-circuit potential. The results of these tests are plotted in Figure 3-2 for comparison with those conducted in the absence of thiosulfate. SCC

Table 3-2. Results of slow strain rate tests of type 316L stainless steel in dilute chloride solutions with the addition of thiosulfate at 95 °C

Solution	Gas	E_{corr} (mV_{SCE})	E_{app} (mV_{SCE})	Current (A)	Initial pH	Final pH	Elong. (%)	Failure Time (h)	Test Results
1,000 ppm Cl^- + 10^{-3} M $Na_2S_2O_3$	CO_2	−232	−175 to 78	10^{-6} to 10^{-5}	8.3	6.5	60.4[a]	176[a]	Ductile failure.
1,000 ppm Cl^- + 10^{-3} M $Na_2S_2O_3$	CO_2	−186	O.C. (−285 to −155)	—	8.3	6.5	64.2[a]	179[a]	Ductile failure.
1,000 ppm Cl^- + 10^{-2} M $Na_2S_2O_3$	CO_2	−209	−183 to 20	10^{-6} to 9×10^{-5}	7.8	5.1	28.4[b]	364[b]	Localized corrosion. No SCC.
1,000 ppm Cl^- + 10^{-2} M $Na_2S_2O_3$	CO_2	−237	O.C. (−238 to −296)	—	7.8	—	No failure	477[b]	Test interrupted. No SCC.
1,000 ppm Cl^- + 10^{-3} M $Na_2S_2O_3$	CO_2	−200	−200	10^{-6}	7.7	5.2	2.51[d]	950[e]	Ductile failure.
1,000 ppm Cl^- + 10^{-2} M $Na_2S_2O_3$	79% N_2 21% O_2	−155	O.C. (−155 to −67)	—	4.0	4.5	No failure	932[e]	Localized corrosion. No SCC.
1,000 ppm Cl^- + 10^{-2} M $Na_2S_2O_3$	79% N_2 21% O_2	−142	−100 to −173	10^{-6} to 1×10^{-3}	4.0	7.5	No failure	932[e]	Localized corrosion. No SCC.
1,000 ppm Cl^- + 10^{-2} M $Na_2S_2O_3$	CO_2	−179	O.C. (−180 to −120)	—	4.0	6.2	69.4[b]	787[b]	Ductile failure[f].

O.C. – Open circuit
a – $\dot{\varepsilon}=1.0\times10^{-6}\ s^{-1}$
b – $\dot{\varepsilon}=2.2\times10^{-7}\ s^{-1}$
c – Notched specimen at extension rate = 7.1×10^{-7} mm/s (2.8×10^{-8} in./s)
d – extension in mm
e – Constant deflection test at 105 percent yield for 476 hr and at 130 percent yield for 456 hr
f – Solution-annealed specimen

did not occur in tests conducted in solutions containing 0.01 mol/L $Na_2S_2O_3$ even though the extension rate was decreased more than 4×, which implies that the severity of the tests was increased with respect to that conducted at the low-thiosulfate concentration. The use of a notched specimen did not lead to crack initiation, even though an O-ring was used to create crevice conditions and a very low-extension rate was applied. No SCC occurred after 950 hr of straining, and the test was, therefore, interrupted.

Two tests were conducted under constant elongation conditions using smooth tensile specimens at the open-circuit and anodic-applied potentials. In these tests, the pH was adjusted to 4.0 by the addition of HCl, and the solutions were purged with synthetic air to attain a higher open-circuit potential. Both specimens were loaded initially up to 105 percent of the nominal yield point. After 476 hr of testing without any signs of crack initiation and growth as indicated by the lack of load relaxation, the load was increased to 130 percent of the yield point. No load relaxation was observed during the subsequent 456-h period, and both tests were then terminated. Localized corrosion was observed, but no cracks were detected on the specimen surfaces.

A final test of this series with the addition of thiosulfate was conducted using a solution-annealed specimen of type 316L SS to evaluate if the solution-annealed material was more susceptible to SCC than that in the mill-annealed condition. As shown in Table 3-2, an elongation to failure of 69.4 percent was obtained in this test, indicating that pure ductile failure occurred as confirmed by stereoscopic examination. The elongation to failure was similar to that obtained for mill-annealed materials in the absence of localized corrosion.

Table 3-3 summarizes the results of the set of tests conducted in various concentrated chloride solutions of different cations using smooth tensile specimens. These solutions were selected to increase the concentration of chloride ions beyond that obtained with NaCl as an electrolyte and to be able to conduct tests under atmospheric pressure at temperatures higher than 100 °C. The initial tests of this set were conducted at 120 °C in 40-percent $MgCl_2$ solution (14.0 molal Cl^-) at the corrosion potential (approximately $-300\ mV_{SCE}$) and at a slightly anodic potential ($-280\ mV_{SCE}$). SCC was observed under both conditions, in which elongation values of 7.4 and 4.6 percent were obtained, respectively. Similar results were obtained at a lower temperature (110 °C) in a less concentrated solution (30-percent $MgCl_2$) in which the chloride concentration was 9.1 molal. In this case again, a decrease in the elongation to failure from 49.4 to 15.2 percent was observed by increasing the potential to slightly anodic values with respect to the open-circuit potential.

Extensive secondary cracking was observed on the side surfaces of these specimens (Figure 3-3), with the exception of the specimen tested at the open-circuit potential in the less concentrated solution in which very few incipient cracks were detected. Fractographic examination revealed that, besides the "cleavage-like" features (Figure 3-4) typical of the transgranular cracking of austenitic SSs in boiling $MgCl_2$ solutions (Scully, 1971), intergranular cracking occurred over a large proportion of the fracture surface (Figure 3-5). An overall view of the fracture surface seems to indicate that cracking initiated transgranularly but propagated mostly in an intergranular fashion through the specimen (Figure 3-6). The proportion of intergranular cracking diminished with the decrease in the severity of the environment, in terms of chloride concentration and temperature, and also with the decrease in potential.

SCC was also observed in ten tests conducted at temperatures ranging from 120 to 95 °C in concentrated LiCl solutions acidified by the addition of HCl, as summarized in Table 3-3. The pattern was similar to that found in $MgCl_2$ solutions at equivalent chloride concentrations and temperatures. SCC occurred under open-circuit conditions, but cracking susceptibility increased significantly with anodic

Table 3-3. Results of slow strain rate tests ($\dot{\varepsilon}=1\times10^{-6}\ s^{-1}$) of type 316L stainless steel in concentrated chloride solutions

Solution	T (°C)	E_{corr} (mV_{SCE})	E_{app} (mV_{SCE})	Current (Amps)	Initial/ Final pH	Elong. (%)	Failure Time (h)	Test Results
14.0 molal Cl^- (40% $MgCl_2$)	120	−311	O.C (−343 to −306)	—	—	7.4	22.9	IGSCC and TGSCC
14.0 molal Cl^- (40% $MgCl_2$)	120	−280	−260 to −275	10^{-5} to 4×10^{-3}	—	4.6	12.4	IGSCC and TGSCC
9.1 molal Cl^- (30% $MgCl_2$)	110	−331	O.C. (−331 to −367)	—	4.9/ 5.9	49.4	138.6	IGSCC and ductile
9.1 molal Cl^- (30% $MgCl_2$)	110	−326	−316 to −360	10^{-5} to 3×10^{-3}	4.9/ 5.9	15.2	44.7	IGSCC and TGSCC
13.9 molal Cl^- (LiCl)	120	−356	O.C. (−345 to −402)	—	1.6/ 1.4	15.6	44.2	TGSCC and IGSCC
13.9 molal Cl^- (LiCl)	120	−353	−322	10^{-6} to 1.0×10^{-3}	1.6/ 2.0	2.6	7.2	TGSCC, some IGSCC
13.9 molal Cl^- (LiCl)	115	−333	O.C. (−312 to −400)	—	3.9/ 6.1	17.0	45.6	SCC, several secondary cracks
13.9 molal Cl^- (LiCl)	100	−328	O.C (−318 to −466)	—	4.0/ 6.4	27.8	78.0	TGSCC, some IGSCC
13.9 molal Cl^- (LiCl)	95	−340	O.C. (−319 to 376)	—	4.1/ 6.4	25.8	73.3	SCC, several secondary cracks
9.1 molal Cl^- (LiCl)	110	−353	O.C. (−353 to −370)	—	2.1/ 6.1	29.4	79.2	TGSCC, IGSCC some ductile
O.C. – open circuit								

Table 3-3. Results of slow strain rate tests ($\dot{\varepsilon}=1\times10^{-6}$ s^{-1}) of type 316L stainless steel in concentrated chloride solutions (cont'd)

Solution	T (°C)	E_{corr} (mV_{SCE})	E_{app} (mV_{SCE})	Current (amps)	Initial/ Final pH	Elong. (%)	Failure Time (h)	Test Results
9.1 molal Cl^- (LiCl)	110	−343	−320 to −340	-1×10^{-5} to 10^{-3}	2.1/ 5.9	13.2	38.3	TGSCC and IGSCC
9.1 molal Cl^- (LiCl)	100	−339	O.C. (−298 to −391)	—	4.0/ 4.6	31.0	87.0	SCC
9.1 molal Cl^- (LiCl)	95	−342	O.C. (−319 to −367)	—	4.0/ 4.4	40.6	117.0	SCC
7.2 molal Cl^- (LiCl)	100	−342	O.C. (−319 to −356)	—	4.0/ 6.2	47.4	135.0	SCC
6.2 molal Cl^- (NaCl)	95	−361	O.C. (−350 to −390)	—	2.6/ —	64.0	177.7	Ductile failure
6.2 molal Cl^- (NaCl)	95	−363	−345 to −380	-1×10^{-5} to 2.0×10^{-3}	2.6/ 7.0	28.8	80.2	Ductile failure/pitting
6.2 molal Cl^- (NaCl)	95	−359	−360 to −380	10^{-7} to 10^{-4}	2.7/ 6.7	35.6[a]	267.2[a]	Ductile failure/pitting
6.2 molal Cl^- (NaCl)	95	−356	−340 to −380	5×10^{-3}	2.7/ 8.2	13.2[a]	104.3[a]	Severe pitting
6.2 molal Cl^- (LiCl)	95	−340	−320 to −348	5×10^{-3}	2.4/ 7.9	10.8[a]	90.3[a]	Severe pitting
6.2 molal Cl^- (LiCl)	95	−347	−294 to −680	-2×10^{-4} to 5×10^{-3}	2.5/ 5.6	56.0[a]	435.1[a]	Ductile failure/pitting

O.C. - open circuit a - $\dot{\varepsilon}=3.6\times10^{-7}$ s^{-1}

Table 3-3. Results of slow strain rate tests ($\dot{\varepsilon}=1\times10^{-6}$ s^{-1}) of type 316L stainless steel in concentrated chloride solutions (cont'd)

Solution	T (°C)	E_{corr} (mV_{SCE})	E_{app} (mV_{SCE})	Current (amps)	Initial/ Final pH	Elong. (%)	Failure Time (h)	Test Results
6.2 molal Cl^- (LiCl)	95	−362	−391 to −355	10^{-6} to 10^{-5}	3.2/ 5.8	30.6[b]	397[b]	Ductile failure/pitting
6.2 molal Cl^- (LiCl)	95	−342	−660 to −330	10^{-6} to 10^{-5}	3.7/ 3.9	36.4[b]	469[b]	Ductile failure/pitting
6.2 molal Cl^- (NaCl)	95	−352	O.C. (−350 to −340)	10^{-6} to 3×10^{-4}	3.2/ 6.8	55.0[b]	650[b]	Ductile failure/pitting
6.2 molal Cl^- (NaCl)	95	−332	−330	10^{-6} to 10^{-3}	3.2/ 7.3	63.4[b]	795[b]	Ductile failure/pitting
6.2 molal Cl^- (NaCl)	95	−347	−280 to −389[c]	2×10^{-5} (Galvanostatic)	4.4/ —	42.4[b]	554.4[b]	Ductile failure/pitting
6.2 molal Cl^- (NaCl)	95	−341	−237 to −374[c]	4×10^{-5} (Galvanostatic)	4.4/ 7.4	31.8[b]	404.5[b]	Ductile failure/pitting

O.C. – open circuit b – $\dot{\varepsilon}=2.2\times10^{-7}$ s^{-1} c – potential variation during galvanostatic test

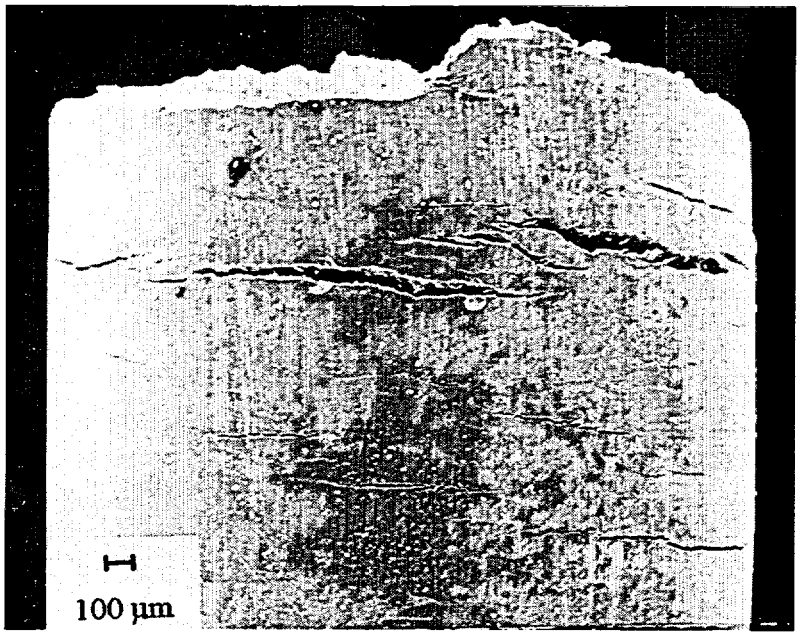

Figure 3-3. Side surface of the type 316L stainless steel specimen tested under open-circuit conditions in 40-percent $MgCl_2$ solution at 120 °C showing the presence of many secondary cracks

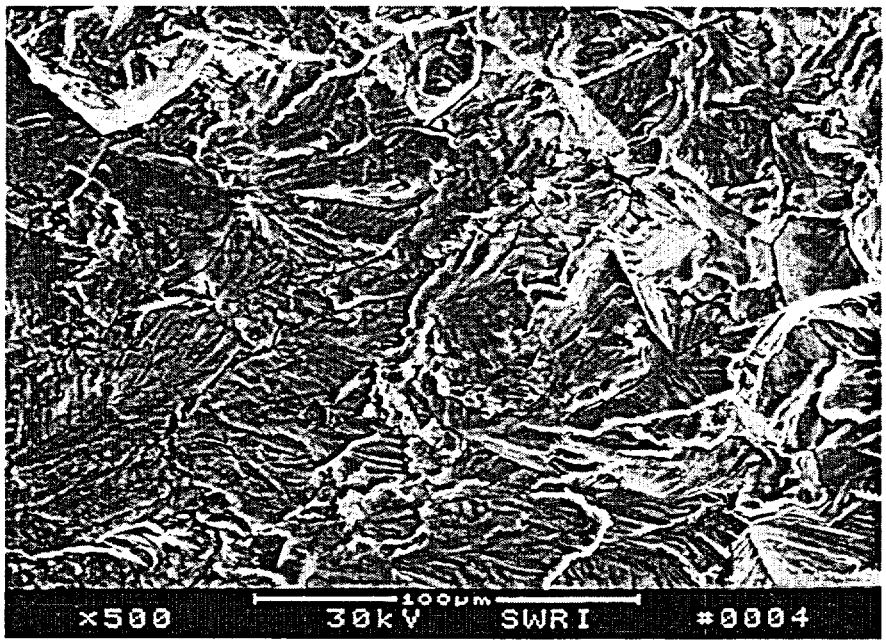

Figure 3-4. Fractograph showing the transgranular stress corrosion cracking area of the type 316L stainless steel specimen tested under open-circuit conditions in 40-percent $MgCl_2$ solution at 120 °C

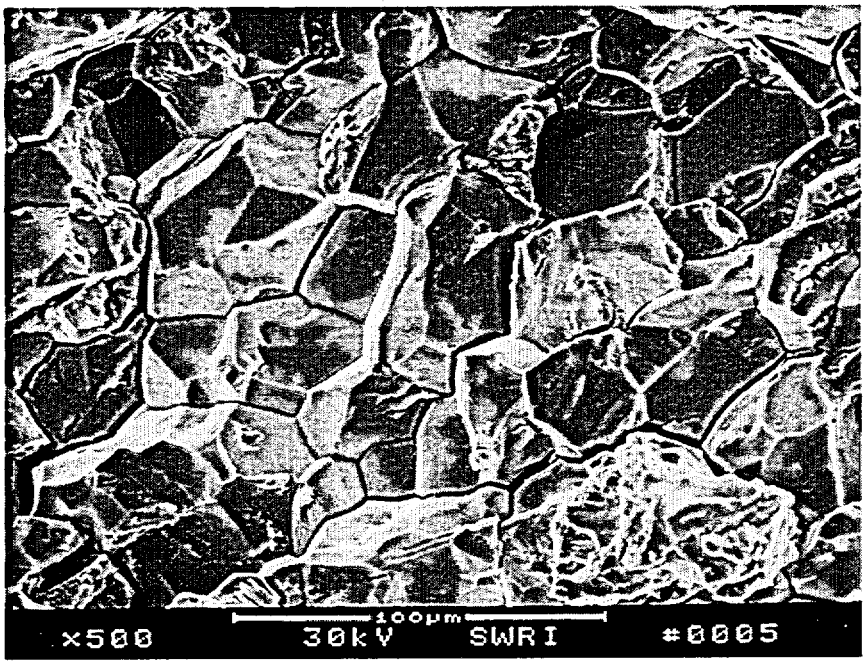

Figure 3-5. Fractograph showing the intergranular stress corrosion cracking area of the type 316L stainless steel specimen tested under open-circuit conditions in 40-percent $MgCl_2$ solution at 120 °C

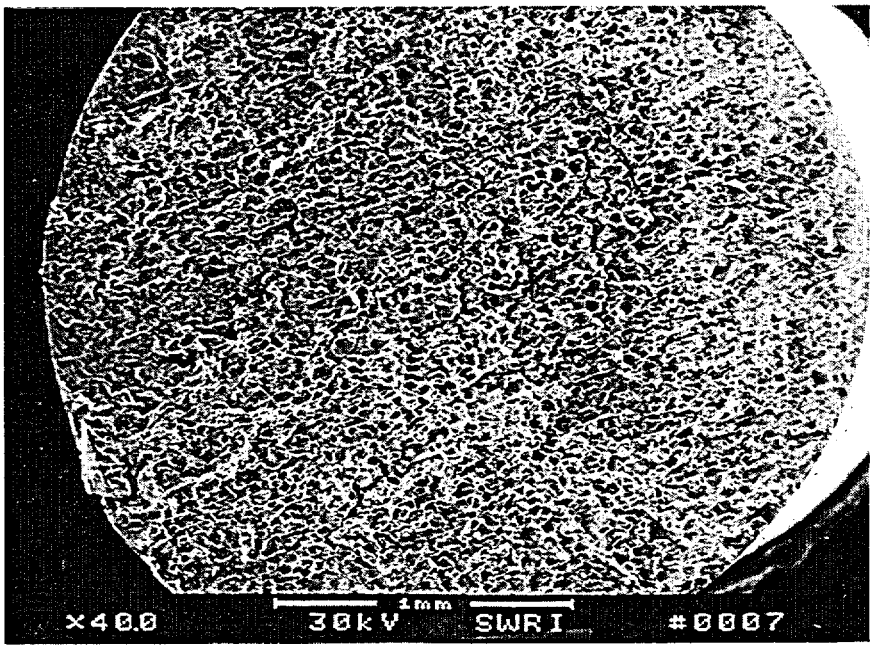

Figure 3-6. Overall fracture surface of type 316L stainless steel specimen tested under open-circuit conditions in 40-percent $MgCl_2$ solution at 120 °C

polarization. These observations were confirmed by fractographic examination. Extensive areas of intergranular and transgranular SCC were observed in these fractographs (Figures 3-7 and 3-8). It appears, however, that the proportion of intergranularly cracked areas was smaller than observed under equivalent conditions in $MgCl_2$ solutions. The susceptibility to SCC, as evaluated from the elongation to failure values and the appearance of the fracture surfaces, decreased with decreasing chloride concentration and temperature.

As shown in Table 3-3, two tests were conducted at 95 °C in a concentrated NaCl solution (6.2 molal Cl^-) in which the pH was adjusted to 2.6 by the addition of HCl. This concentration was chosen because it is close to the solubility of NaCl at 95 °C, which is equal to 6.7 molal (Linke, 1965), with the purpose of comparing the behavior of type 316L SS in NaCl with that in LiCl solutions. An elongation to failure of 64 percent was obtained under open-circuit conditions, that decreased to 28.8 percent at a slight anodic potential. The potential was diminished by about 25 mV during the course of the test in order to avoid pitting corrosion, which was controlled by maintaining the current below 1 mA. Whereas the specimen tested at the corrosion potential exhibited ductile failure, the one tested at an anodic potential exhibited a relatively unusual, flat topography in a significant fraction of the fracture surface. However, no "quasi-cleavage" features, typical of transgranular SCC, or the grain faces characteristic of intergranular SCC were noted in the fractographs. Some irregular pits, around 100 μm in diameter, were observed on the side surfaces. The complete absence of secondary cracks, however, indicates that SCC did not occur in these solutions.

Four additional tests were conducted using a lower strain rate at 95 °C to compare the behavior in NaCl solutions with that in LiCl solutions at an equivalent chloride concentration of 6.2 molal with the pH adjusted to 2.5±0.2. The strain rate was decreased to 2.2×10^{-7} s^{-1} to increase the sensitivity of the technique. However, as shown in Table 3-3, no SCC was observed in these tests. Severe pitting occurred in two of these tests, causing premature failure of the specimens. In the remaining two tests ductile failure predominated but was accompanied by pitting corrosion.

In a final set of tests conducted at 95 °C in solutions containing a chloride concentration of 6.2 molal, the strain rate was decreased to 2.2×10^{-7} s^{-1}, which is more than 4× lower than in the initial tests. No SCC was observed in this series of tests in which open-circuit and anodic conditions were tested under both potentiostatic and galvanostatic control. Indeed, galvanostatic tests were used in an attempt to avoid the occurrence of pitting corrosion by limiting the applied current to values typical of the passive range. This galvanostatic control was reflected in corrosion potentials during straining ranging from -350 to -380 mV_{SCE}, which are just below E_p. Nevertheless, pitting corrosion still occurred accompanying the ductile failure. No signs of cracks were observed on the side surfaces of these specimens.

Several stress-versus-elongation curves obtained in some of the tests conducted in concentrated LiCl solutions are plotted for comparison in Figure 3-9. The different curves represent the range of behavior from severe SCC to ductile failure with minor pitting corrosion. The significant decrease in ductility promoted by the application of an anodic overpotential of only 30 mV with respect to the corrosion potential is clearly seen in the curves for the 9.1 molal LiCl solution. The slow relaxation of the load, caused by the propagation of cracks, is particularly noticeable in this test. On the other hand, a very high elongation to failure, close to 55 percent, accompanied by a sudden drop in the load characterizes the predominantly ductile behavior in the 6.2 molal LiCl solution. The results of the tests conducted in concentrated LiCl solutions are presented as a function of chloride concentration and

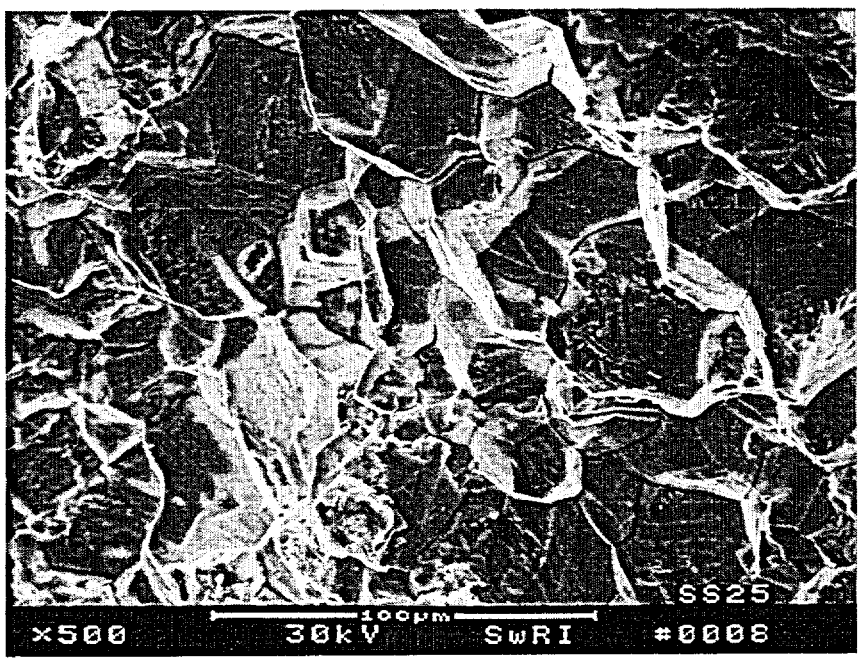

Figure 3-7. Fractograph showing the intergranular stress corrosion cracking area of the type 316L stainless steel specimen tested under an anodic potential in 13.9 molal LiCl solution at 120 °C

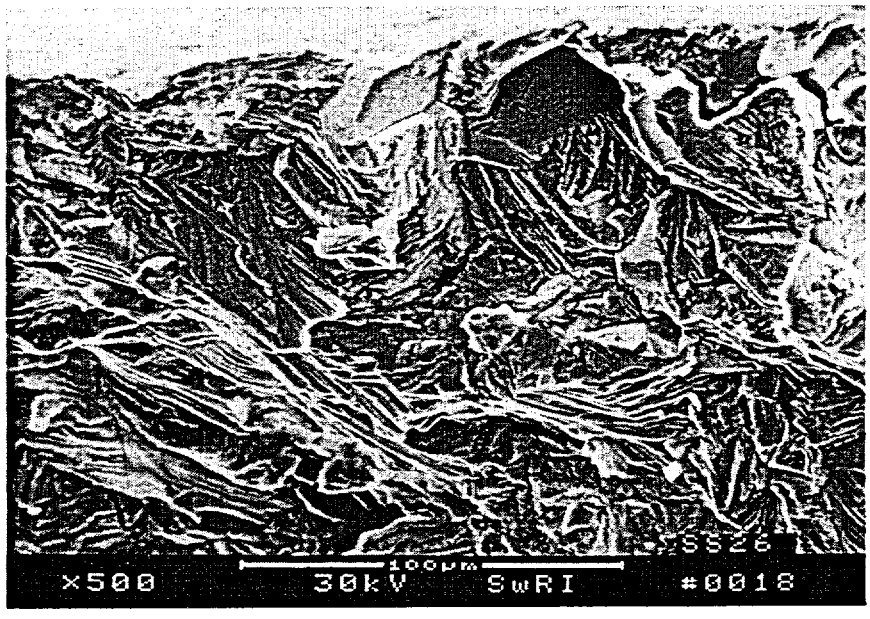

Figure 3-8. Fractograph showing the transgranular stress corrosion cracking area at the edge of the fracture surface in the type 316L stainless steel specimen tested under open-circuit conditions in 13.9 molal LiCl solution at 120 °C

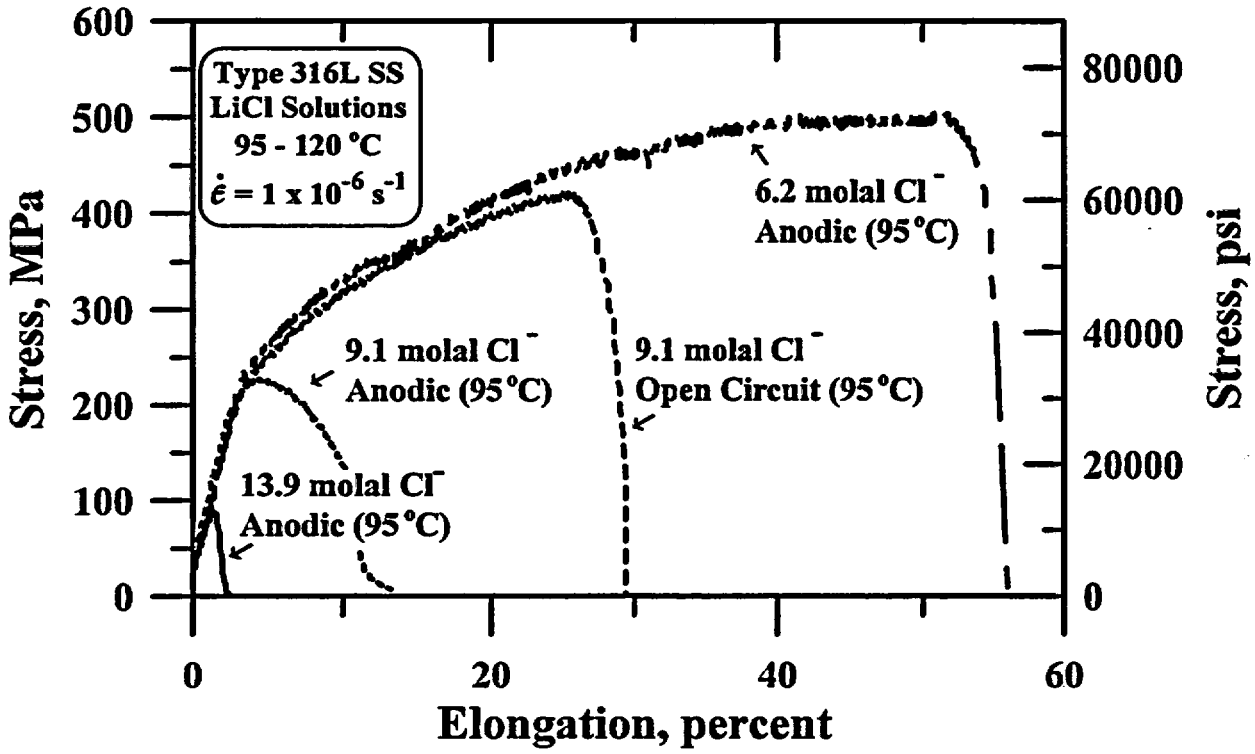

Figure 3-9. Stress versus elongation curves obtained in slow strain rate tests of type 316L stainless steel in concentrated LiCl solutions at temperatures ranging from 95 to 120 °C

temperature in Figures 3-10 and 3-11, respectively, to illustrate the important effect of these variables on the elongation to failure. A significant decrease in the elongation to failure at chloride concentrations greater than 6.2 molal, which levels off at higher concentrations, is shown in Figure 3-10. The results of the slow strain rate tests conducted in concentrated chloride solutions are summarized in Figure 3-12 in terms of potential and chloride concentration.

An additional set of tests was conducted at 95 °C in deaerated 1 M NaCl solution with the pH adjusted to 4.0 by the addition of HCl. In these tests, a crevice-forming device made of PFA tubing and a PTFE holder was clamped on the gage length of the smooth tensile specimens to promote the development of crevice corrosion and eventually the initiation of cracks. After two initial tests, one at the open-circuit potential and the other at a slightly anodic potential, the strain rate was decreased from $1\times10^{-6}\ s^{-1}$ to $2.2\times10^{-7}\ s^{-1}$ to allow more exposure time for crack initiation in the crevice. Although crevice attack in the form of small pits occurred in the occluded area covered by the PFA tubing, all the specimens tested failed by ductile fracture, as indicated in Table 3-4. No SCC occurred in the last three tests of this set as shown in Table 3-4, even though galvanostatic conditions were applied with the expectation that widespread pitting corrosion would be avoided by controlling the current, and initiation of cracks would become the favorable anodic process. Only in the test in which the applied current was the lowest (1.0×10^{-5} amps) were very minor cracks detected in the gage length within the crevice area. However, the area was predominantly attacked by pitting corrosion, and apparently the cracks did not grow sufficiently to promote failure by SCC.

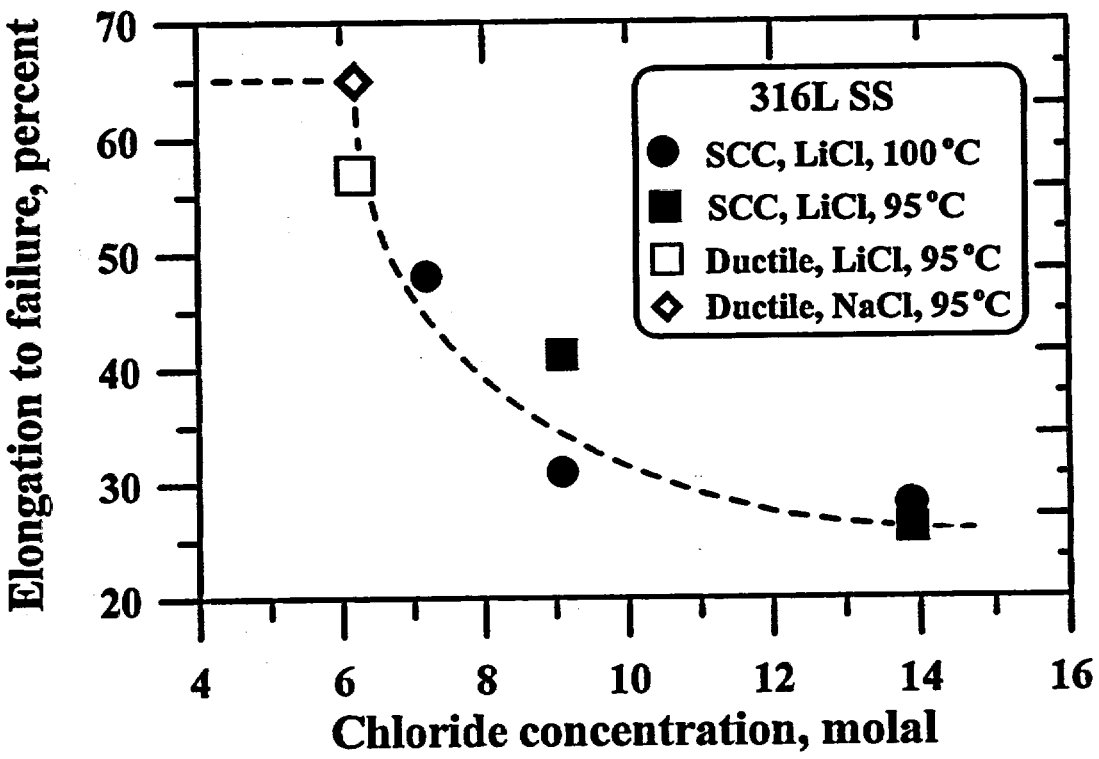

Figure 3-10. Elongation to failure as a function of chloride concentration for slow strain rate tests of type 316L stainless steel in LiCl solutions at 95 and 100 °C under open-circuit conditions

In the last set of slow strain rate tests, smooth tensile specimens of type 316L SS were tested in concentrated NaCl solutions containing 0.01 M $Na_2S_2O_3$ with the pH adjusted to 4.0 by the addition of HCl, as shown in Table 3-5, in which data for alloy 825 are also included. SCC of mill-annealed type 316L SS was observed at the open-circuit potential, which was found to be -390 mV_{SCE}, a value approximately 40 mV lower than that in the absence of thiosulfate, and also at low-anodic potentials (-420 to -390 mV_{SCE}). The elongation to failure in these two tests, 12.2 and 18.0 percent, was very low, indicating a significant susceptibility to SCC in this environment. To avoid the occurrence of pitting corrosion, the potential in the test conducted potentiostatically was maintained during most of the test time below the open-circuit potential, which may explain the increased elongation to failure obtained in this test with respect to that under open-circuit conditions. Figures 3-13 and 3-14 show the typical appearance of the fracture surfaces observed in these tests, in which the coexistence of intergranular and transgranular cracking can be clearly noted. For comparison, a solution-annealed specimen of type 316L SS was tested at the open-circuit potential in the same solution. The elongation to failure, 11.4 percent, was similar to that for the mill-annealed specimen.

In summary, SCC of type 316 SS was not observed in slow strain rate tests at chloride concentrations lower than 7.2 molal in the absence of thiosulfate. In the presence of 0.01 M thiosulfate, SCC was observed in solutions containing 5.8 molal Cl^- but not in 0.028 molal Cl^- (1,000 ppm).

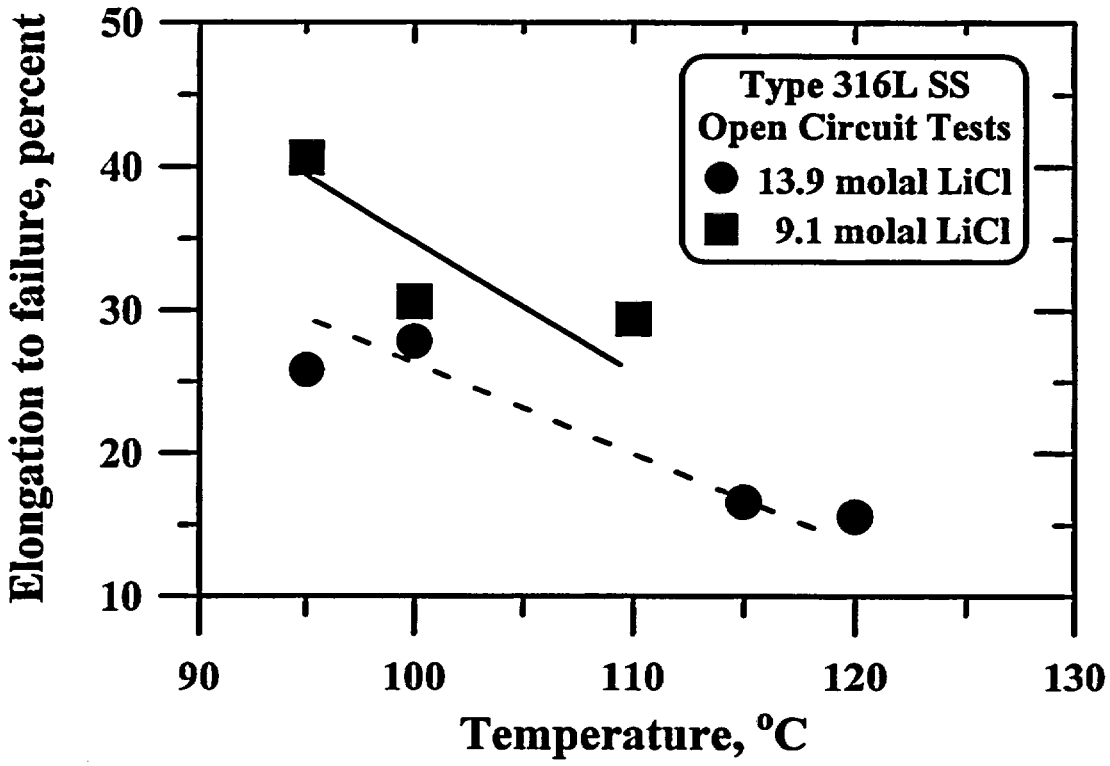

Figure 3-11. Elongation to failure as a function of temperature for slow strain rate tests of type 316L stainless steel in 9.1 and 13.9 molal LiCl solutions under open-circuit conditions

3.1.2 Alloy 825

In contrast to the case of type 316L SS, no SCC occurred in alloy 825, when tested in 5.8 molal NaCl solution containing 0.01 M $Na_2S_2O_3$ at 95 °C, at the open-circuit or at an anodic-applied potential (Table 3-5). Ductile failure prevailed, but it was accompanied by pitting corrosion at the vapor/solution interface. SCC was not observed in a notched specimen of alloy 825 tested at an even lower extension rate. This test was initiated under open-circuit conditions, but a slight anodic potential was applied later in the course of the test, after 908 hr of straining, in an attempt to promote crack initiation. Straining was interrupted after 1,104 hr corresponding to a nominal extension of 2.62 mm, without any signs of crack initiation, as shown in Table 3-5.

The results of slow strain rate tests of alloy 825 in concentrated chloride solutions are presented in Table 3-6 and summarized in Figure 3-15. In this figure, E_p and E_{rp}, as measured on unstressed specimens of alloy 825 using a scan rate of 0.167 mV/s (Sridhar et al., 1993a), are plotted as a function of chloride concentration to indicate the location of the open-circuit or applied potentials used in the slow strain rate tests. The E_p line is a regression fit line, whereas the E_{rp} curve is drawn through the lowest value of this parameter measured at each chloride concentration. It should be noted that above 4 molal Cl^-, E_{rp} deviates significantly from the linear dependence on the logarithm of chloride concentration observed in more dilute chloride solutions. As shown in Figure 3-15, SCC was observed,

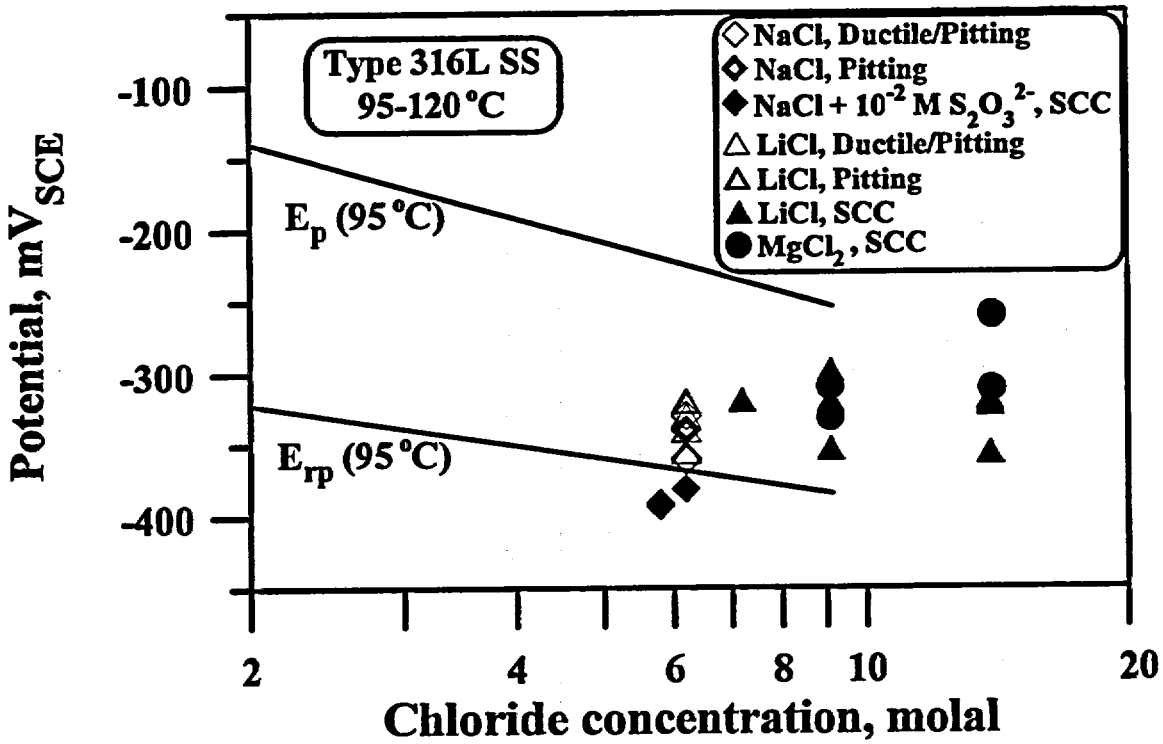

Figure 3-12. Results of slow strain rate tests of type 316L stainless steel in concentrated chloride solutions ($MgCl_2$, LiCl, and NaCl) in terms of potential and chloride concentrations at temperatures ranging from 95 to 120 °C. Failure modes after testing are indicated.

both at an anodic potential as well as at the E_{corr} only in 40-percent $MgCl_2$ solution (14.0 molal Cl^-) at 120 °C. The elongation to failure was 44 percent at the E_{corr} (approximately -270 mV_{SCE}) and decreased to 36 percent at a slightly anodic potential (-260 mV_{SCE}) whereas the elongation to failure corresponding to a purely ductile fracture was approximately 60 percent.

No SCC was observed in LiCl solutions at chloride concentrations of 9.1 molal at 110 °C under both open-circuit and anodic-applied potentials. Also, SCC did not occur in the same solution in another test in which a circumferentially notched specimen was used and the strain rate was decreased 5× with respect to that applied for smooth tensile specimens. This test was conducted under open-circuit conditions (-290 mV_{SCE}). The test was interrupted after 757 hr of straining corresponding to 1.96 mm extension. In this test, the specimen was unloaded and removed from the electrochemical cell to be examined. No signs of SCC were detected in the notch area.

All observations were confirmed by fractographic examination of the failed smooth tensile specimens using the SEM. Several thumbnail-shaped areas exhibiting transgranular quasi-cleavage features were observed along the periphery of the fracture surface of the alloy 825 specimens tested in $MgCl_2$ solution, both at the open-circuit as well as the anodic-applied potential. One of these areas is shown at high magnification in Figure 3-16 confirming the occurrence of SCC. The appearance of numerous secondary cracks on the side surface of these specimens is illustrated in Figure 3-17. The coalescence of

Table 3-4. Results of slow strain rate tests ($\dot{\varepsilon}=2.2 \times 10^{-7}\ s^{-1}$) of type 316L stainless steel in deaerated 1 M NaCl solution at 95 °C using specimen with crevice-forming device

E_{corr} (mV_{SCE})	E_{app} (mV_{SCE})	Current (A)	Initial pH	Final pH	Elong. (%)	Failure Time (h)	Test Results
−265	−260 to −210	-10^{-6} to 2.8×10^{-5}	3.9	8.0	63.2[a]	176.5[a]	Ductile failure, small pits in crevice
−245	O.C. (−219 to −373)	—	3.9	8.0	60.4[a]	173.0[a]	Ductile failure, small pits in crevice
−256	−256 to −150	-10^{-6} to 2.0×10^{-4}	3.9	7.9	35.0	421.0	Ductile failure with pitting
−339	−250 to −150[b]	1×10^{-5} (Galvanostatic)	4.0	7.3	38*	470*	Ductile failure with pitting
−259	−256 to −141[b]	$5\text{-}7\times10^{-5}$ (Galvanostatic)	4.0	7.9	34*	420*	Ductile failure with pitting
−287	−275 to −214[b]	3×10^{-5} (Galvanostatic)	4.0	7.7	42.2	508.0	Crevice corrosion/pitting and ductile failure

O.C. - open circuit a - $\dot{\varepsilon}=1\times10^{-6}\ s^{-1}$ b - potential variation during galvanostatic test * - approximate values

Table 3-5. Results of slow strain rate tests ($\dot{\varepsilon}=2.2\times10^{-7}\ s^{-1}$) of type 316L stainless steel and alloy 825 in concentrated chloride solutions with the addition of thiosulfate at 95 °C

Alloy	Solution	E_{corr} (mV_{SCE})	E_{app} (mV_{SCE})	Current (A)	Initial/ Final pH	Elong. (%)	Failure Time (h)	Test Results
Mill-annealed Type 316L SS	5.8 molal NaCl + 0.01 M $Na_2S_2O_3$	−393	O.C. (−386 to −450)	—	—/ —	12.2	155	IGSCC, TGSCC
Mill-annealed Type 316L SS	5.8 molal NaCl + 0.01 M $Na_2S_2O_3$	−391	−420 to −391	10^{-6} to 2×10^{-4}	—/ —	18.0	241	IGSCC, TGSCC
Solution-annealed Type 316L SS	6.2 molal NaCl + 0.01 M $Na_2S_2O_3$	−381	O.C. (−358 to −438)	—	4.0/ 4.9	11.4	145	IGSCC, TGSCC
Alloy 825	5.8 molal NaCl + 0.01 M $Na_2S_2O_3$	−336	O.C. (−296 to −381)	—	3.4/ 3.8	47.6	613	Pitting/ductile failure. (Pits at vapor/ solution interface.)
Alloy 825	5.8 molal NaCl + 0.01 M $Na_2S_2O_3$	−339	−325 to −344	-3×10^{-6} to 3×10^{-4}	3.4/ 3.8	34.6	431	Pitting/ductile failure. (Pits at vapor/ solution interface.)
Alloy 825	5.8 molal NaCl + 0.01 M $Na_2S_2O_3$	−330	O.C. and −0.322	-1×10^{-5} to 10^{-4}	3.4/ —	2.62[a]	1,104[a]	No SCC

O.C. – open circuit a – Notched specimen; extension rate of 7.1×10^{-7} mm/s; elongation in mm; test interrupted without failure

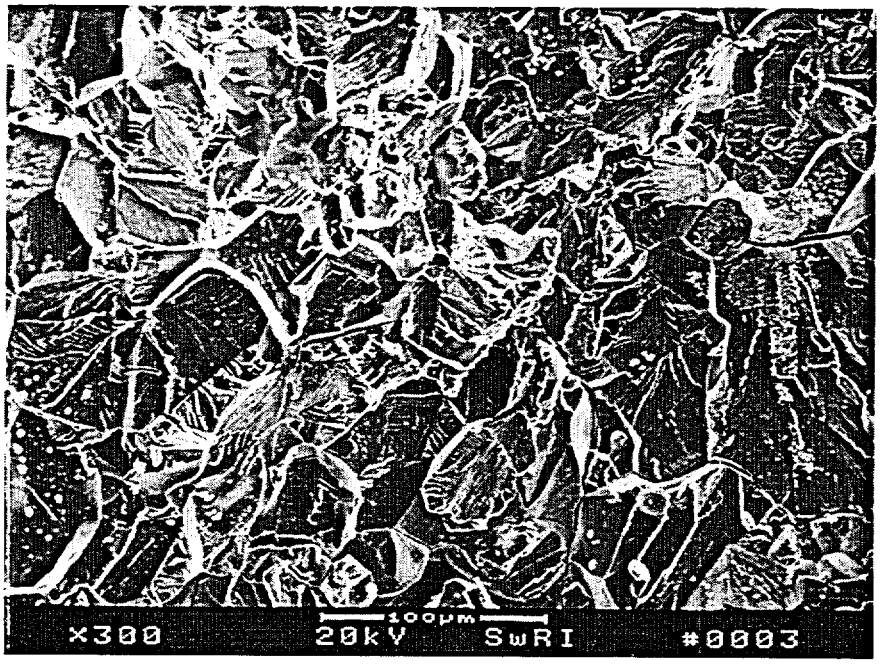

Figure 3-13. Fractograph showing a predominantly transgranular cracked area in the fracture surface of the type 316L stainless steel specimen tested under open-circuit conditions in 5.8 molal NaCl solution with the addition of 0.01 M $Na_2S_2O_3$ at 95 °C

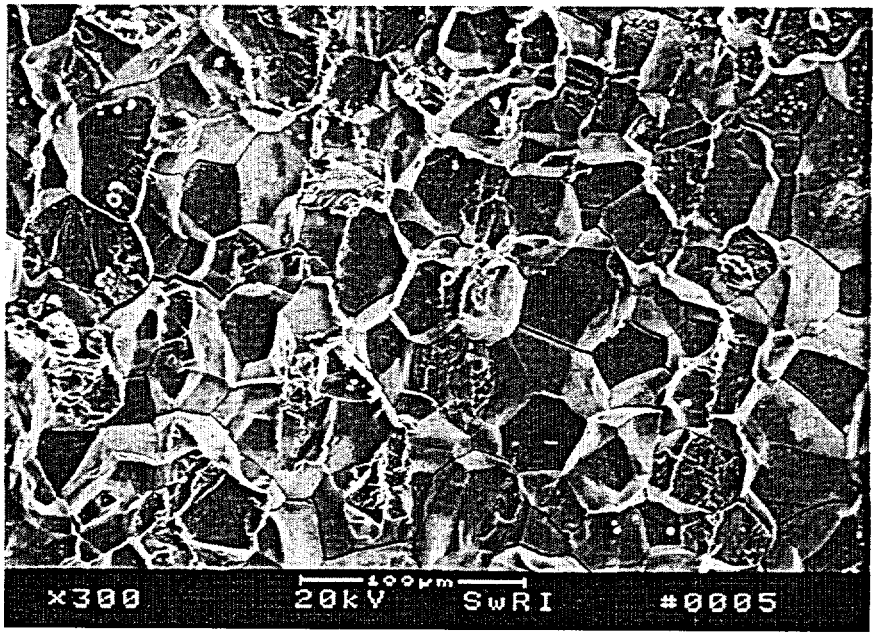

Figure 3-14. Fractograph showing the intergranular cracked area in the fracture surface of the type 316L stainless steel specimen tested under open-circuit conditions in 5.8 molal NaCl solution with the addition of 0.01 M $Na_2S_2O_3$ at 95 °C

Table 3-6. Results of slow strain rate tests ($\dot{\varepsilon}=1\times10^{-6}\ s^{-1}$) of alloy 825 in concentrated chloride solutions

Solution	T (°C)	E_{corr} (mV_{SCE})	E_{app} (mV_{SCE})	Current (A)	Initial /Final pH	Elong. (%)	Failure Time (h)	Test Results
9.1 molal Cl^- (LiCl)	110	−297	−272 to −303	-2×10^{-6} to 7×10^{-5}	2.0/ 2.4	60.6	170.0	Pitting/ductile failure. Pits at V/S interface.
9.1 molal Cl− (LiCl)	110	−254	O.C. (−226 to −323)	—	2.0/ 1.8	62.6	179.0	Pitting/ductile failure. Pits at V/S interface.
9.1 molal Cl^- (LiCl)	110	−290	O.C. (−295 to −243)	—	2.0/ 3.0	1.96[a]	757.0[a]	No SCC, some small pits, corrosion in notched area.
14 molal Cl^- (40% $MgCl_2$)	120	−262	−257 to −316	-2×10^{-6} to 3×10^{-4}	—/ —	36.4	102.5	TGSCC, many secondary cracks.
14 molal Cl^- (40% $MgCl_2$)	120	−272	O.C. (−258 to −334)	—	—/ —	43.6	124.9	TGSCC, many secondary cracks.
a – Notched specimen; extension rate of 7.2×10^{-7} mm/s (2.8×10^{-8} in./s); extension in mm; test interrupted without failure. V/S: vapor solution								

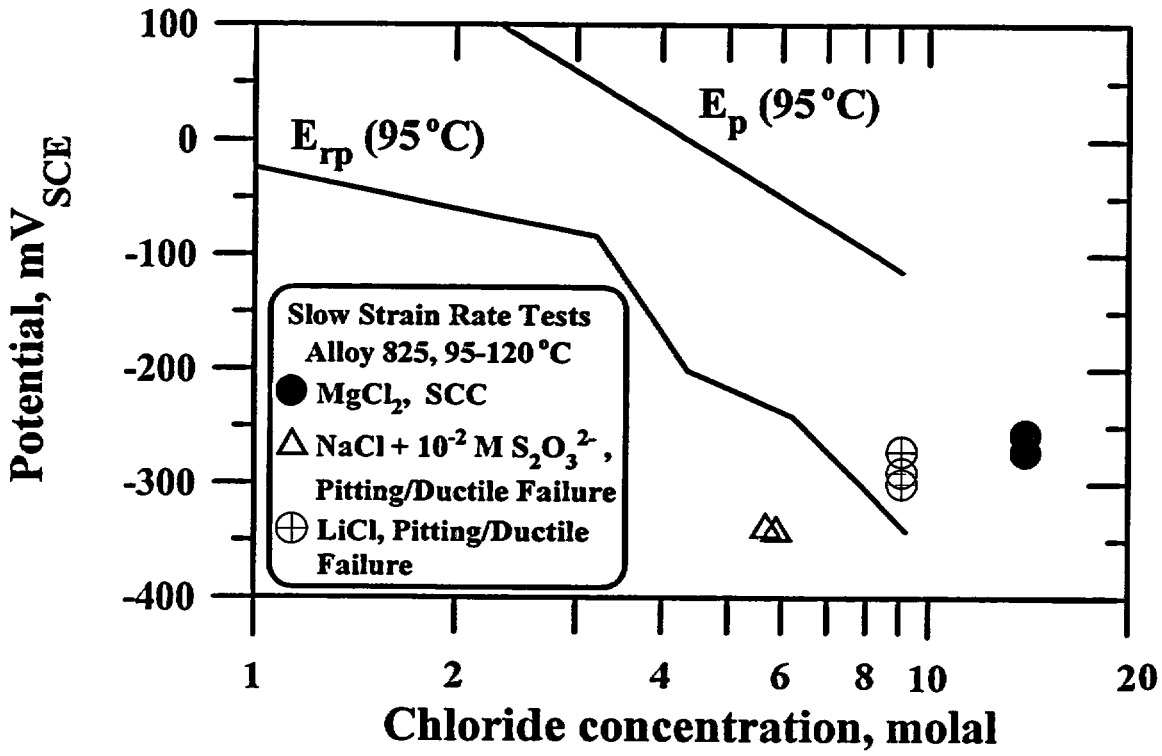

Figure 3-15. Results of slow strain rate tests of alloy 825 in concentrated chloride solutions ($MgCl_2$, LiCl, and NaCl), with and without the addition of thiosulfate, in terms of potential and chloride concentrations at temperatures ranging from 95 to 120 °C

deep, slightly branched cracks, growing in different planes, led to the generation of an extremely uneven fracture surface.

Ductile failure promoted by coalescence of microvoids was observed in all the remaining tests of alloy 825. Signs of pitting corrosion were also detected on the fracture surface, although the dominant feature in the fractographs was the presence of dimples associated with ductile failure. Pits were also observed on the specimen surface, mainly at the vapor/solution interface.

No relevant slow strain rate test could be conducted under potentiostatic conditions at higher anodic potentials than those tested, because the occurrence of pitting corrosion became the dominant process accompanying the ductile failure. To avoid the occurrence of pitting corrosion, the potential was diminished by a few millivolts during the course of some tests in order to maintain the current well below 1 mA. Taking into consideration the resistance to SCC exhibited by alloy 825 in 5.8 molal NaCl solution even in the presence of sodium thiosulfate, no attempt was made to study the effect of lower chloride concentration on the susceptibility to SCC.

In summary, SCC of alloy 825 was not observed in chloride solutions using the slow strain rate technique over a wide range of chloride concentrations, except in 40-percent $MgCl_2$ at 120 °C, which corresponds to 14 molal Cl^-.

Figure 3-16. Scanning electron microscope fractograph showing the transgranular stress corrosion cracking area of the alloy 825 specimen fractured in a slow strain rate test at an applied potential of $-260\ mV_{SCE}$ in 40-percent $MgCl_2$ solution at 120 °C

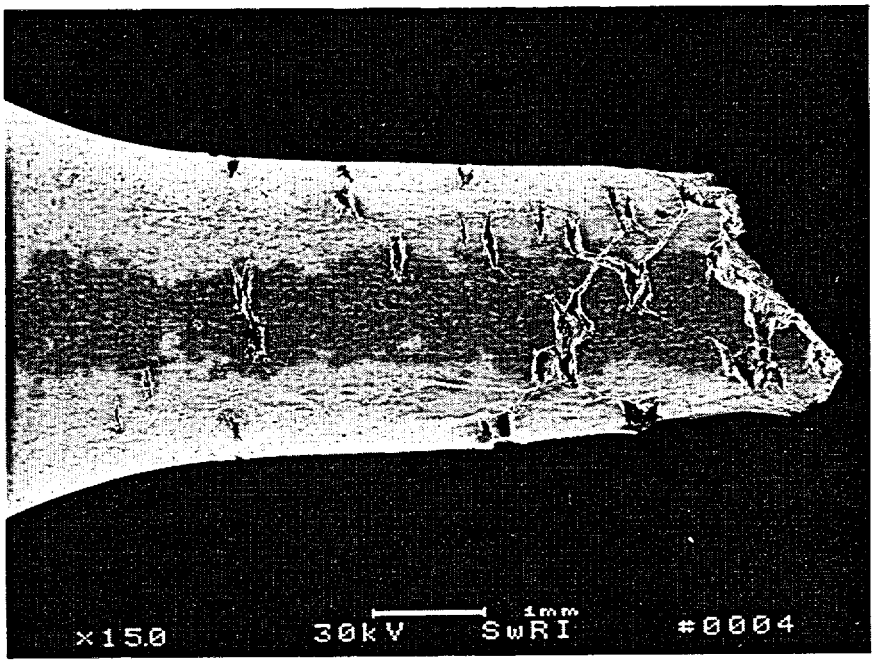

Figure 3-17. Side surface of the alloy 825 specimen tested at an applied potential of $-260\ mV_{SCE}$ in 40-percent $MgCl_2$ solution at 120 °C

3.2 CONSTANT DEFLECTION TESTS

3.2.1 Type 316L Stainless Steel

Table 3-7 summarizes the results of constant deflection tests using U-bend specimens of type 316L SS in dilute chloride solutions (1,000 ppm Cl^-) at 95 °C. After 528 hr (22 d) of testing, a crack was observed at an applied potential about 40- to 80-mV anodic to the open-circuit potential (-180 mV_{SCE}), but not under open-circuit conditions in a companion specimen. The crack was observed on the leg of the U-bend specimen above the vapor/solution interface. In a subsequent test conducted for three consecutive periods of 504, 672, and 672 hr, corresponding to a total of 1,848 hr (77 d), no cracking was detected on the specimens at either open-circuit or anodic-applied potentials after the first and second exposure periods, as indicated in Table 3-7. The predominant phenomenon was the occurrence of localized corrosion in the form of small pits, mainly located in the legs of the U-bends above the vapor/solution interface. However, cracks were observed after the third exposure period in both specimens on the leg above the vapor/solution interface, as indicated in Figure 3-18. Figure 3-19 shows the appearance after the third exposure period of one of the main cracks on the outer surface of the leg, just below the location of the bolt, in the specimen tested at the anodic potential. A cross-sectional metallography, obtained in the same location (Figure 3-20), reveals the transgranular and branched path of several cracks.

SCC was observed in most of the specimens tested in dilute chloride solutions (1,000 ppm Cl^-) with the addition of 0.01 M of thiosulfate. Cracking was found to be more severe in the presence of thiosulfate, even though the addition of this species decreased the corrosion potential by approximately 100 mV in solutions purged with the N_2/O_2 gas mixture simulating air. Additional details are indicated in Table 3-7. As in the case of plain chloride solutions, cracks were always found above the vapor/solution interface despite the fact that the legs are the less stressed part of the U-bend specimens. SCC was observed in the test with the shortest duration (288 hr), even at the open-circuit potential. In this test, however, the corrosion potential was higher (-130 V_{SCE}) because no gas was bubbled into the solution. No SCC was detected in the specific case of the specimen tested under open-circuit conditions for a testing period of 528 hr, in which the N_2/O_2 gas mixture was bubbled into the solution. In contrast, SCC occurred in the specimen held at an anodic potential. In the final test summarized in Table 3-7, SCC was detected in specimens exposed at both open-circuit and anodic potentials after a total exposure time of 1176 hr, although no cracking was observed during the initial test period that extended for 504 hr.

Table 3-8 summarizes the results of the tests conducted in concentrated chloride solutions. SCC was observed in all the U-bend specimens with the exception of one specimen tested in 6.2 molal NaCl at the open-circuit potential, in which pitting corrosion instead of SCC was observed in the bend area. LiCl solutions appear to be marginally more aggressive in terms of promoting SCC, because SCC was observed in all the tests conducted in solution containing at least a chloride concentration equal to 5.8 molal, regardless of the application of an anodic overpotential. In the case of NaCl solutions, no SCC was detected under open-circuit conditions at 6.2 molal, but this test lasted only 288 hr. On the other hand, the addition of thiosulfate or the application of an anodic overpotential promoted cracking in the same time interval. In this concentrated chloride solution, the addition of thiosulfate did not have any significant effect on the corrosion potentials, which were about -350 ± 20 mV_{SCE} in most of these tests. The results of the constant deflection tests are plotted in terms of potential in Figure 3-21, for both dilute and concentrated chloride solutions, to indicate the potentials at which SCC was observed in relation to E_{rp} and E_p.

Table 3-7. Summary of U-bend test results for type 316L stainless steel in dilute chloride solutions at 95 °C

Solution	Purging Gas	E_{corr} (mV_{SCE})	E_{app} (mV_{SCE})	Current (A)	Initial pH	Final pH	Test Time (h)	Results
1,000 ppm Cl^- as NaCl	79% N_2 21% O_2	−130	O.C. (−130 to −230)	—	4.0	—	528	No SCC, shallow pits above V/S interface
1,000 ppm Cl^- as NaCl	79% N_2 21% O_2	−180	−140 to −100	10^{-4} to 10^{-6}	4.0	—	528	SCC on leg above V/S interface
1,000 ppm Cl^- as NaCl	79% N_2 21% O_2	−110 −180[a] −240[b]	O.C.	—	4.3 4.1[a] 4.5[b]	— 5.8[a] 8.3[b]	504 672[a] 672[b]	No SCC No SCC, shallow pits on leg above V/S interface[a] SCC on leg above V/S interface[b]
1,000 ppm Cl^- as NaCl	79% N_2 21% O_2	−70 −190[a] −170[b]	−55 to 5 −100[a] −100[b]	10^{-7} to 10^{-6} 10^{-6} to 10^{-5} 10^{-6} to 10^{-4}	4.3 4.1[a] 4.5[b]	— 5.8[a] 8.3[b]	504 672[a] 672[b]	No SCC, shallow pits on leg No SCC, pits on leg in vapor phase[a] SCC on leg above V/S interface[b]
1,000 ppm Cl^- as NaCl + 0.01 M $Na_2S_2O_3$	—	−130	O.C.	—	—	—	288	SCC on leg above V/S interface and pits at V/S interface
1,000 ppm Cl^- as NaCl + 0.01 M $Na_2S_2O_3$	—	−130	−20 to −110	10^{-5} to 10^{-6}	—	—	288	SCC on leg above V/S interface
1,000 ppm Cl^- as NaCl + 0.01 M $Na_2S_2O_3$	79% N_2 21% O_2	−270	O.C. (−270 to −200)	—	4.0	—	528	No SCC, pits above V/S interface
1,000 ppm Cl^- as NaCl + 0.01 M $Na_2S_2O_3$	79% N_2 21% O_2	−270	−220	10^{-6}	4.0	—	528	SCC at top of leg above bolt and V/S interface
1,000 ppm Cl^- as NaCl + 0.01 M $Na_2S_2O_3$	79% N_2 21% O_2	−240 −240[a]	O.C.	—	4.9 4.6[a]	— 8.3[a]	504 672[a]	No SCC, shallow pits on leg SCC on leg under bolt washer above V/S interface[a]
1,000 ppm Cl^- as NaCl + 0.01 M $Na_2S_2O_3$	79% N_2 21% O_2	−210 −140[a]	−150 to 0 −100[a]	10^{-7} to 10^{-6} 10^{-6} to 10^{-5}[a]	4.9 4.6[a]	— 8.3[a]	504 672[a]	No SCC, shallow pits on leg SCC on leg above V/S interface and pits on leg[a]

O.C. – open circuit a – Second test period after initial period of 504 hr b – Third test period after 1,176 hr of testing V/S – vapor/solution

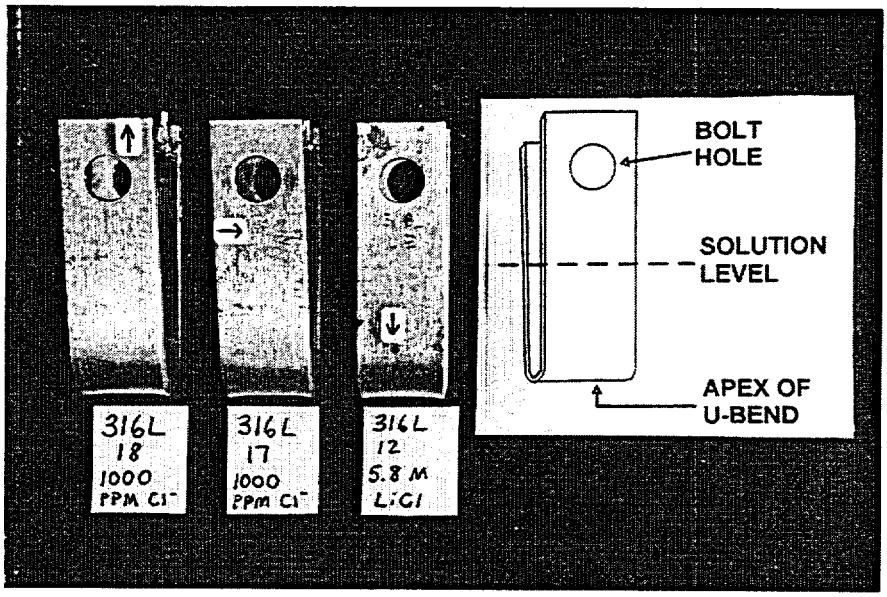

Figure 3-18. Photograph showing the location of cracks in U-bend specimens of type 316L stainless steel tested in dilute (1848 hr) and concentrated (528 hr) chloride solutions at 95 °C

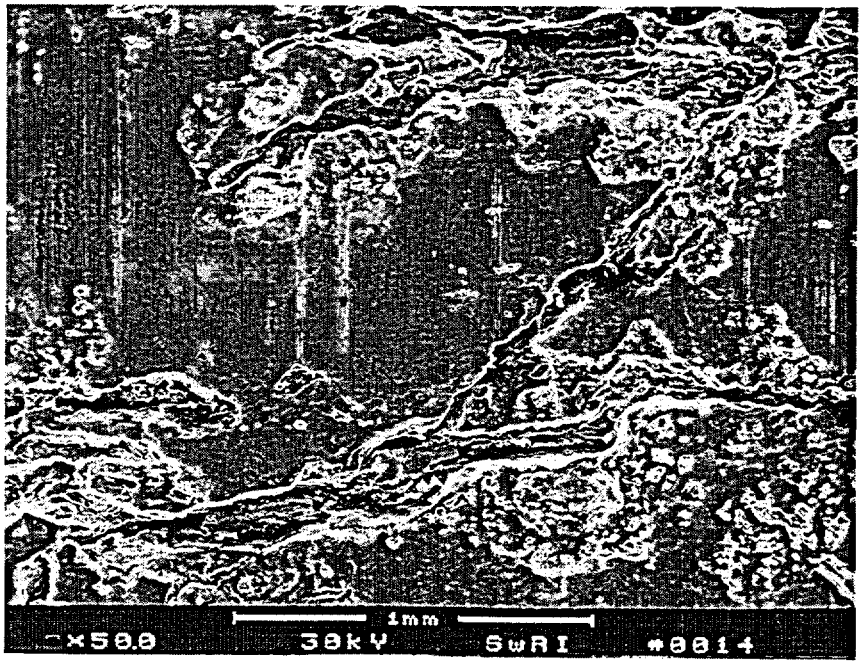

Figure 3-19. Appearance of the cracks observed above the vapor/solution interface on the leg of the type 316L stainless steel specimen tested for 1848 hr in the solution containing 1,000-ppm chloride at 95 °C

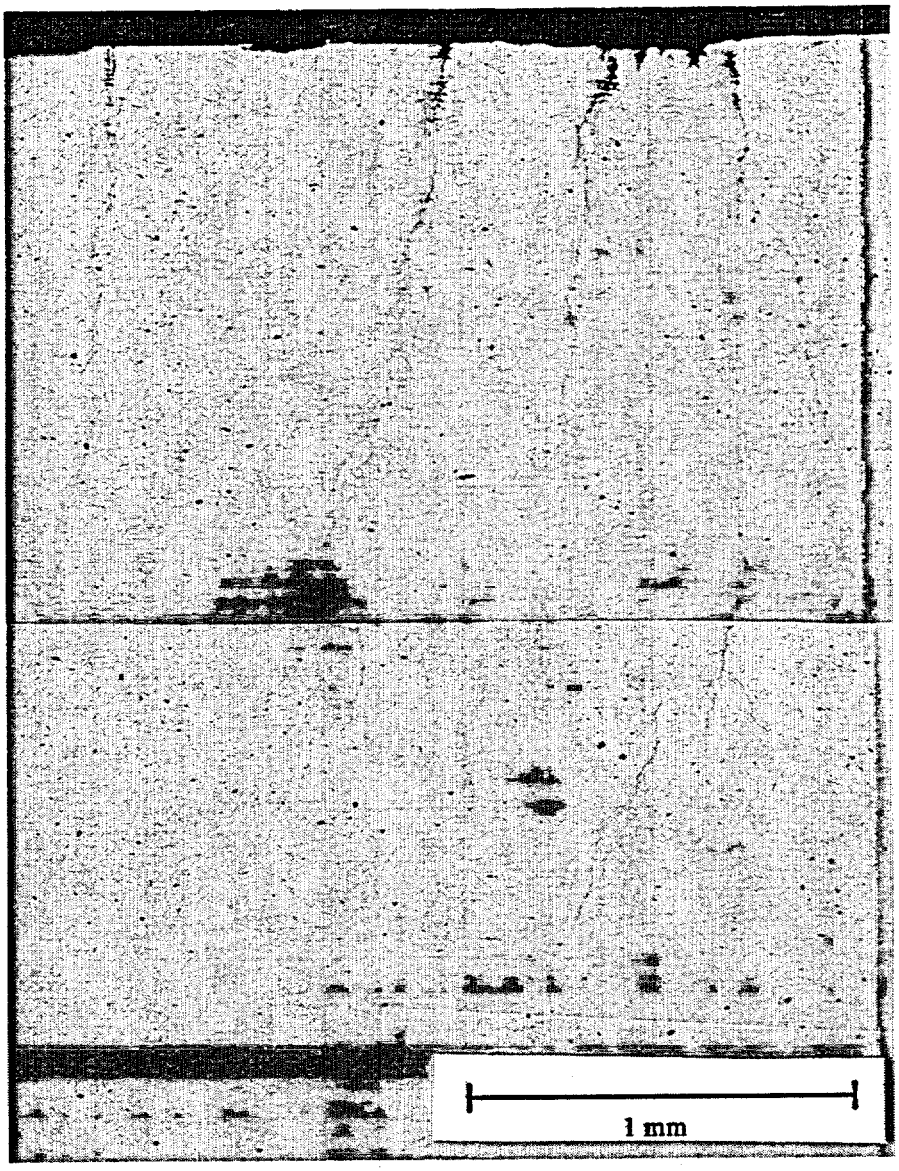

Figure 3-20. Metallography illustrating the initiation and propagation of cracks on the leg of the type 316L stainless steel specimen tested for 1848 hr in the solution containing 1,000-ppm chloride at 95 °C

Table 3-8. Summary of U-bend test results for type 316L stainless steel in concentrated chloride solutions at 95 °C

Solution	Purging Gas	E_{corr} (mV_{SCE})	$E_{applied}$ (mV_{SCE})	Current (A)	Initial pH	Test time (h)	Results
5.8 molal Cl^- as LiCl	79% N_2 21% O_2	−340	O.C.	—	4.0	528	SCC on bend and leg
5.8 molal Cl^- as LiCl	79% N_2 21% O_2	−340	−290	10^{-4}	4.0	528	SCC on bend and leg, pits on bend
9.03 molal Cl^- as LiCl	—	−350	O.C.	—	4.0	288	SCC on bend and leg
9.03 molal Cl^- as LiCl	—	−350	−320	10^{-5} to 10^{-3}	4.0	288	SCC on bend and leg
5.94 molal Cl^- as NaCl	79% N_2 21% O_2	−340	O.C.	—	4.0	528	SCC around pit on bend
5.94 molal Cl^- as NaCl	79% N_2 21% O_2	−350	−350 to −300	10^{-4}	4.0	528	SCC on bend and leg, pits on bend
6.2 molal Cl^- as NaCl	—	−390	O.C.	—	4.0	288	Pit on bend
6.2 molal Cl^- as NaCl	—	−390	−480 to −340	10^{-5} to 10^{-3}	4.0	288	SCC on leg
6.2 molal Cl^- as NaCl + 0.01 M $Na_2S_2O_3$	—	−350	O.C.	—	4.0	288	SCC on bend and leg
6.2 molal Cl^- as NaCl + 0.01 M $Na_2S_2O_3$	—	−350	−340	10^{-5} to 10^{-4}	4.0	288	SCC on bend and leg, some shallow pits
O.C. - open circuit							

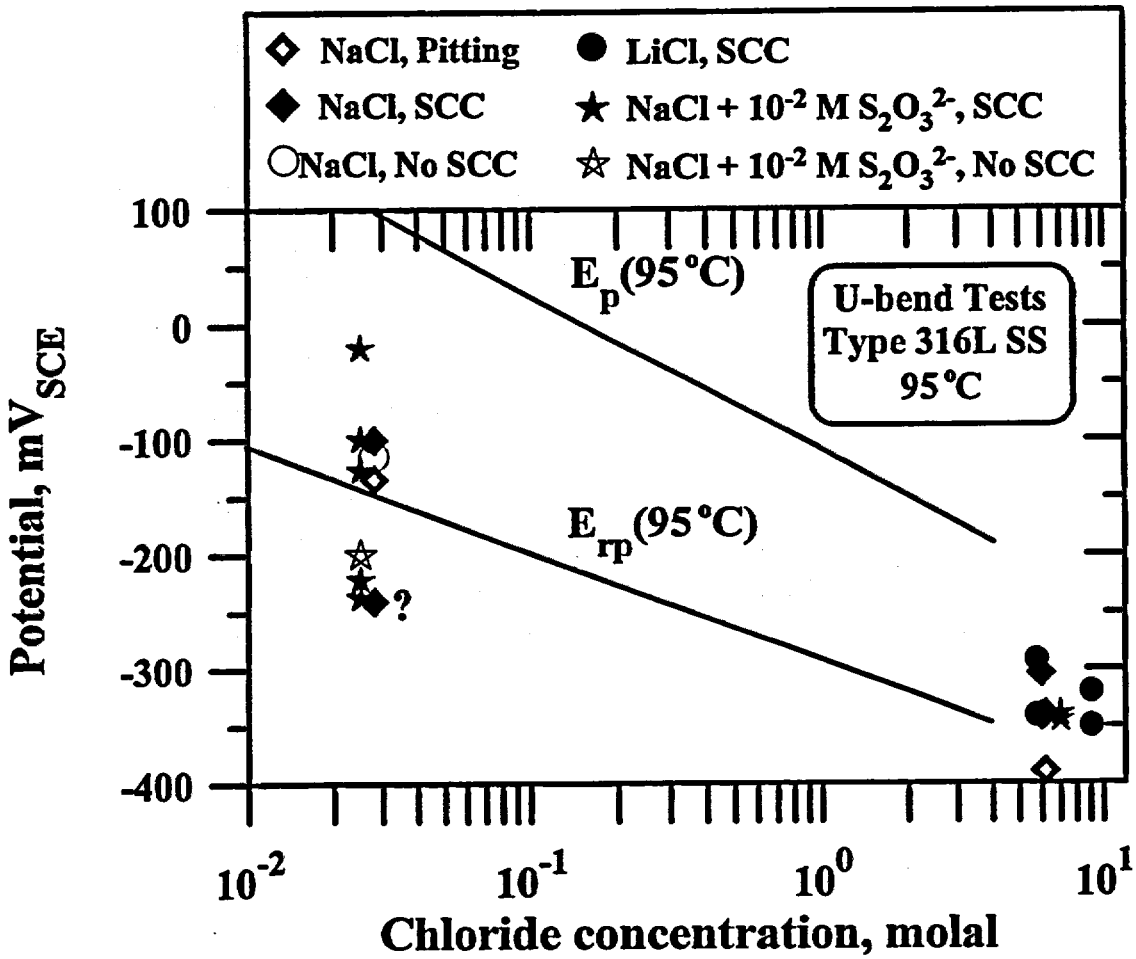

Figure 3-21. Results of constant deflection tests using U-bend specimens of type 316L stainless steel in chloride solutions, with and without the addition of thiosulfate, in terms of potential and chloride concentrations at 95 °C

Figure 3-22 shows the appearance of the cracks in a specimen tested in 5.8 molal LiCl solution at the open-circuit potential. A cross-sectional metallography of the specimen tested in the same solution at an anodic-applied potential is shown in Figure 3-23 to illustrate the distribution of cracks initiated at the outer surface in the apex of the U-bend.

3.2.2 Alloy 825

Table 3-9 summarizes the results of constant deflection tests using U-bends specimens of alloy 825 in concentrated chloride solutions (pH 4.0) at 95 °C, with chloride concentrations ranging from 5.8- to 9.0-molal. No SCC was observed in any of the 11 U-bend specimens tested, in some cases for a total testing time of 4,536 hr (189 d). The time interval for specimen examination was usually 672 hr (28 d). Certain specimens were exposed to alternate cycles of full immersion in the concentrated

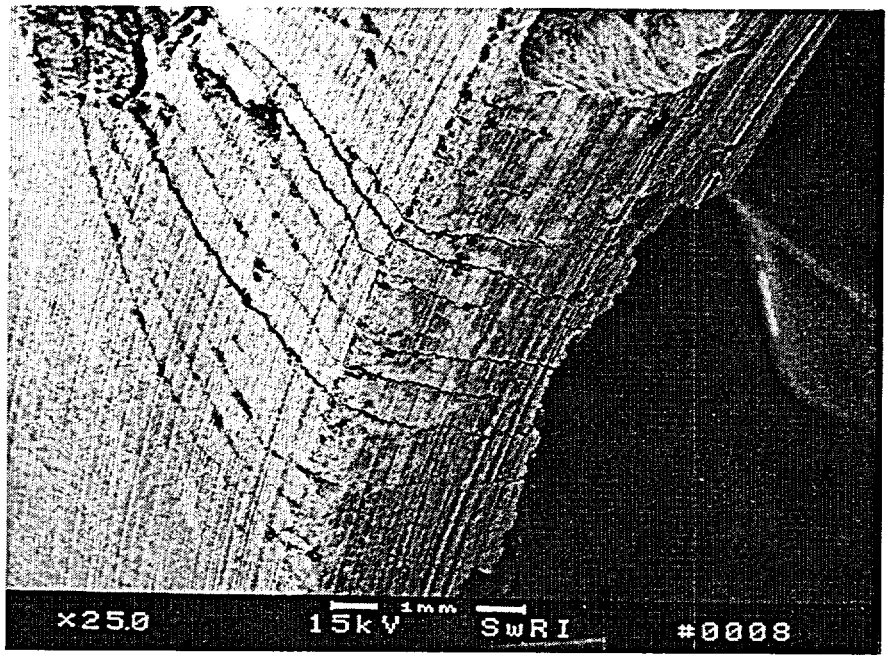

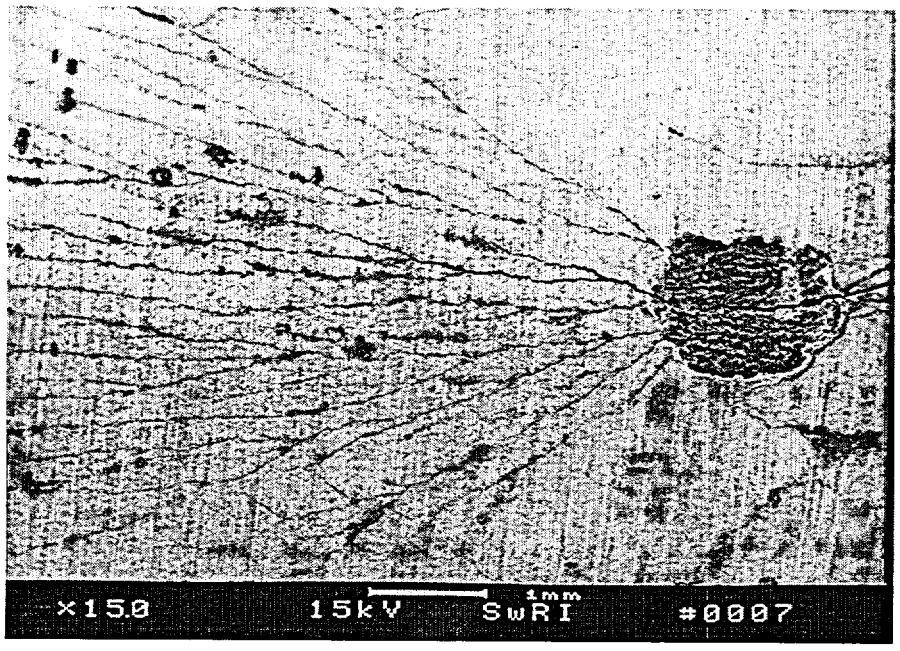

Figure 3-22. Appearance of the cracks observed on the U-bend specimen of type 316L stainless steel tested in 13.9 molal LiCl solution at 95 °C: (a) close to the apex of the U-bend; (b) on the side surface

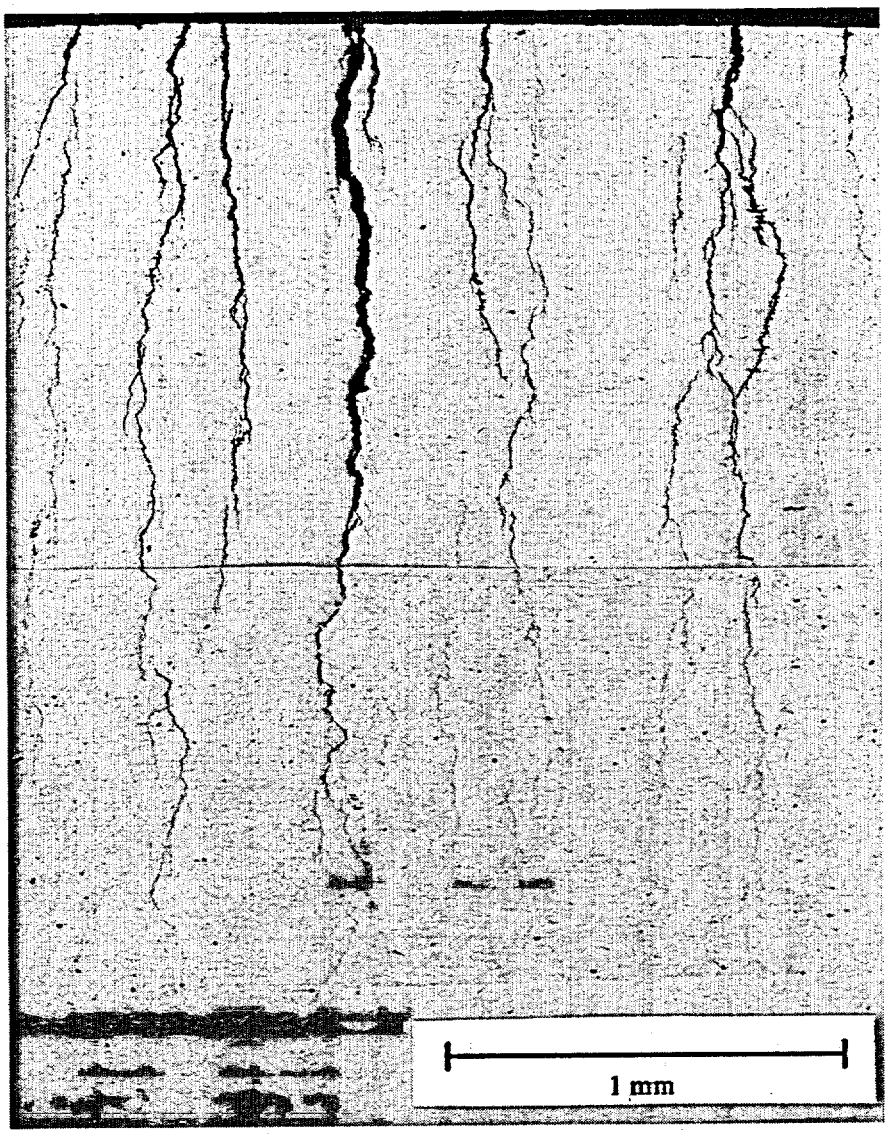

Figure 3-23. Metallography illustrating the initiation and propagation of cracks on the type 316L stainless steel specimen tested in 13.9 molal LiCl solution at 95 °C

Table 3-9. Summary of U-bend test results for alloy 825 in concentrated chloride solutions at 95 °C

Spec. No.	Solution	E_{corr} (mV_{SCE})	E_{app} (mV_{SCE})	Current (A)	Initial pH	Final pH	Test Time (h)	Results
1	6.2 molal Cl^- as NaCl	−170 to −270	O.C.	—	4.2 ±0.5	6.3±0.3	4536	No SCC
2	6.2 molal Cl^- as NaCl	−160	−160	-10^{-7} to 10^{-4}	3.8	—	504	No SCC, large pit on specimen leg
3	5.8 molal Cl^- as LiCl	−260	O.C.	—	4.5±0.6	6.3±0.2	4536	No SCC
4	5.8 molal Cl^- as LiCl	−220	−220	10^{-6} to 10^{-3}	3.4	—	504	No SCC, large pit near apex of specimen
5	6.2 molal Cl^- as NaCl	−270 to −180	−260 to −170	10^{-6} to 10^{-5}	4.2±1.3	5.8	1344	No SCC, localized corrosion
6	5.8 molal Cl^- as LiCl	−260 to −230	−250 to −220	10^{-6} to 10^{-4}	4.7±0.7	6.3±0.2	4032	No SCC
7	9.0 molal Cl^- as LiCl	−300 to −260	−290 to −260	-6×10^{-5} to 2×10^{-4}	4.3±0.1	—	3360	No SCC, pits above and below V/S interface
8	9.0 molal Cl^- as LiCl	−300 to −260	O.C.	—	4.3±0.1	—	3360	No SCC, pits above and below V/S interface
9	6.2 molal Cl^- as NaCl	−300 to −280	−260 to −330	-10^{-5} to 4×10^{-4}	4.1±0.6	6.5±0.2	2688	No SCC
10	5.8 moles Cl^- as LiCl	−310 to −260	O.C	—	4.9±0.4	6.0±0.2	2688	No SCC
11	5.8 moles Cl^- as LiCl	−310 to −250	−300 to −320	-10^{-5} to 2×10^{-4}	4.9±0.4	6.0±0.2	2688	No SCC

O.C. - open circuit V/S - vapor/solution

solutions, followed by exposure to the vapor phase just above the solution/vapor interface. However, no SCC was detected under these conditions. For example, Specimens 1 and 3 were exposed for a total of seven 28-day periods. After an initial 28-day period in which Specimen 3 was immersed in the solution, it was exposed to the vapor phase for the remaining testing time. Specimen 1 was immersed in the solution in periods 1 and 5 and exposed to the vapor phase for the remaining times. Specimens tested under fully immersed conditions for 504 hr (21 d) in both NaCl and LiCl solutions containing 6.0 molal Cl^- at potentials slightly anodic to the open-circuit potential exhibited localized corrosion mostly in the form of small pits located mainly in the legs of the U-bend above the vapor/solution interface. However, these pits did not give rise to cracks upon further exposure.

The results of all the U-bend tests of alloy 825 are plotted in Figure 3-24 to indicate the location of the potentials used in the tests with respect to E_p and E_{rp}. It is seen that, within the range of chloride concentrations tested, no SCC occurred above or below E_{rp}.

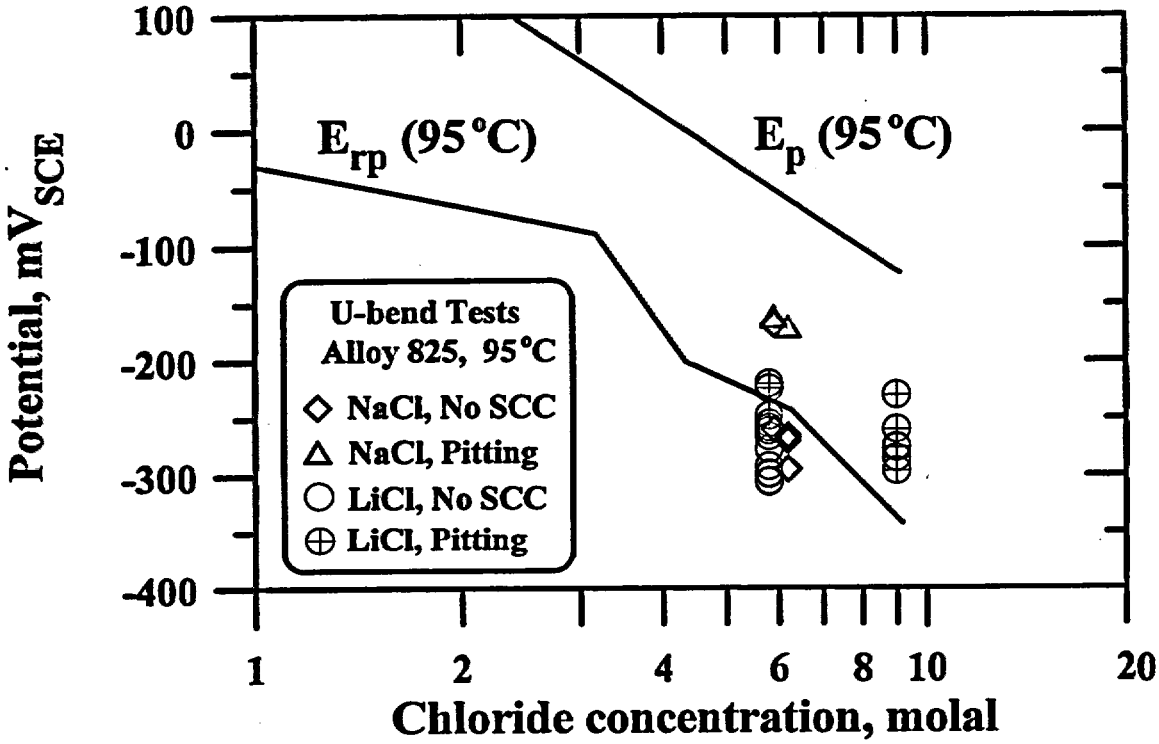

Figure 3-24. Results of constant deflection tests using U-bend specimens of alloy 825 in concentrated chloride solutions in terms of potential and chloride concentration at 95 °C

4 DISCUSSION

4.1 STRESS CORROSION CRACKING OF TYPE 316L STAINLESS STEEL

The results plotted in Figure 3-12 clearly indicate that mill-annealed type 316L SS failed by SCC in slow strain rate tests when exposed to $MgCl_2$ and LiCl solutions at chloride concentrations equal to or greater than 7.2 molal and temperatures above 100 °C. Although SCC was observed under open-circuit conditions, it was significantly enhanced at slightly anodic potentials. As shown in Figure 3-6, the fracture surfaces exhibited a relatively large proportion of intergranularly cracked area in addition to the transgranular features typical of the SCC of annealed, nonsensitized austenitic SS in concentrated chloride-containing solutions. The important effects of chloride concentration and temperature on the SCC susceptibility, as reflected in the elongation to failure values, are shown in Figures 3-10 and 3-11. A significant decrease in these values is observed above 7.2 molal of chloride and temperatures above 95 °C.

Several authors (Takano, 1974; Stalder and Duquette, 1977; Manfredi et al., 1987; Duffo et al., 1988) have reported the simultaneous occurrence of transgranular and intergranular SCC of type 304 SS in slow strain rate tests conducted in concentrated $MgCl_2$ or LiCl solutions at temperatures above 90 °C. The proportion of intergranular to transgranular SCC changes with chloride concentration, temperature, potential, and strain rate, but it is complicated to establish a well-defined pattern as a function of these variables. It appears, however, that the tendency to intergranular SCC increases with decreasing chloride concentration, temperature, and potential, and also with increasing strain rate. Although no similar studies have been conducted with type 316L SS, Okada et al. (1971) have suggested, by studying the SCC behavior of types 304 and 316 SSs, and Fe-16Cr-15Ni-xMo (x=1,2,4) alloys in hot $CaCl_2$ solutions, that the fracture mode became intergranular with higher Mo content. This was attributed by Okada et al. (1971) to the improved corrosion resistance of the alloys brought about by the higher Mo content, which parallels the effect of decreasing corrosivity of the solutions as a result of lower chloride concentrations and temperatures.

On the contrary, as also shown in Figure 3-12 and in more detail in Table 3-3, SCC did not occur in plain NaCl solutions in which the chloride concentration was 6.2 molal. This is close to the maximum concentration attainable in NaCl due to solubility limitations. The same results were obtained in LiCl solutions of equivalent chloride concentration. These results indicate that under the experimental conditions used in these tests, particularly in terms of temperature and strain rate, no SCC can be promoted regardless of the cation at chloride concentrations equal to or lower than 6.2 molal, even at acidic pHs. It should be noted, however, as shown in Table 3-3, that in most of these tests the pH changes from values close to 2.5 before the test to values higher than 6.0 at the end of the test, presumably due to the generation of hydroxide ions at the counterelectrode as a consequence of the reduction of water. However, this explanation is not completely satisfactory because the pH increase was also observed in some tests conducted under open-circuit conditions. It is possible that this increase in pH may render the environment less aggressive in terms of the susceptibility to SCC. In these tests, both open-circuit and applied potentials are within the range defined by the pitting potential, E_p, and the repassivation potential, E_{rp}. The corrosion potential for all these tests, in which N_2 was bubbled into the solution, was on average $-350\ mV_{SCE}$ with a standard deviation of 10 mV. This potential is very close to the extrapolated value of E_{rp} for a chloride concentration of 6.2 molal (Figure 3-12).

The occurrence of SCC of austenitic SSs is expected in neutral, chloride-containing solutions above 80 °C in the low end of this potential range, just above E_{rp} (Cragnolino and Sridhar, 1992; Tamaki et al., 1990; Tsujikawa et al., 1994). Instead of SCC, the dominant failure mode was ductile failure accompanied by pitting corrosion. Since Beavers and Koch (1992) have claimed that the inability to reproduce the SCC of austenitic SSs in dilute chloride solutions using slow strain rate tests may be due to the use of relatively high-extension rates, the strain rate was decreased by almost 3× from 1×10^{-6} to 3.6×10^{-7} s^{-1} in specific tests, as indicated in Table 3-3. Nevertheless, cracks were not initiated, and it was found very difficult to avoid the occurrence of pitting as the predominant phenomenon in this chloride concentration range. Although the potentials selected were approximately 100 mV lower than the extrapolation of the line representing the dependence of E_p with chloride concentration, which defines the electrochemical conditions for pit nucleation in potentiodynamic scans, pitting corrosion was observed on all of these specimens (Table 3-3 and Figure 3-12), after an initiation time of several hours.

The addition of thiosulfate to the NaCl solutions promoted SCC at a slightly lower chloride concentration (5.8 molal) both at the open-circuit and anodic-applied potentials, as shown in Figure 3-12 and Table 3-5. The elongation to failure was almost identical for both mill-annealed and solution-annealed specimens tested under open-circuit conditions (≈ -385 mV_{SCE}), and the fracture surface exhibited transgranular and intergranular cracking (Figures 3-13 and 3-14). SCC occurred in the presence of thiosulfate despite that the corrosion potential was approximately 35 mV lower than that in plain chloride solutions and, therefore, below the extrapolation of the E_{rp} line plotted in Figure 3-12. This effect of thiosulfate can be attributed to the fact that E_{rp} as measured in plain chloride solutions decreases significantly by the addition of thiosulfate. Indeed, Nakayama et al. (1993) have observed that the repassivation potential for crevice corrosion, E_{rcrev}, of type 304 SS decreased by approximately 400 mV when 10 ppm $S_2O_3^{2-}$ was added to a solution containing 100 ppm Cl^-, corresponding to a $S_2O_3^{2-}/Cl^-$ molar ratio of 0.032.

Tsujikawa et al. (1993) reported similar SCC results as those discussed above for solution-annealed type 316L SS in 20-percent NaCl solution (4.3 molal) containing 0.001 to 0.1 M $Na_2S_2O_3$ (pH 4.0) at 80 °C. These authors conducted slow strain rate tests at a strain rate of 2.0×10^{-6} s^{-1} and constant load tests at initial applied stresses higher than 1.3 σ_y, where σ_y is the yield strength of the alloy. However, Tsujikawa et al. (1993) only observed the occurrence of transgranular cracking.

As summarized in Table 3-2, ductile fracture was the single failure mode, even in the presence of thiosulfate, at a lower chloride concentration (1,000 ppm). No SCC was observed in these tests regardless of the increase in thiosulfate concentration, the decrease in strain rate, the application of an anodic potential, or the use of a notched specimen with an O-ring to promote crevice conditions. The $S_2O_3^{2-}/Cl^-$ molar ratio was varied from 0.035 to 0.35 in this set of tests (Table 3-2), which seems to be the appropriate ratio to have a minimum in the curves of E_p and E_{rcrev} as a function of thiosulfate concentration, as demonstrated for type 304 SS by Newman et al. (1982) and Nakayama et al. (1993), respectively. It was expected, although never observed, that cracks could be initiated from the bottom of incipient pits, produced by the localized breakdown of the oxide film during straining. It is well known that pitting corrosion of austenitic stainless steel such as types 304, 304L, and 316L initiates at MnS inclusions (Szklarska-Smialowska, 1986). Furthermore, the presence of crevice geometries introduced to promote crack initiation, through the localized modification of the environment expected in the occluded region, did not lead to the nucleation of cracks. Lott and Alkire (1989) and Alkire and Lott (1989) have shown that the anodic dissolution of MnS inclusions generates $S_2O_3^{2-}$ ions. These species,

in conjunction with chloride, promote initiation of crevice corrosion at induction times that decrease with potential, crevice gap, and areal density of inclusions. It was hypothesized that the exposure time available in slow strain rate tests, limited by the occurrence of ductile failure, was not long enough to facilitate such environmental modification, and therefore, crack initiation. However, as shown in Table 3-2, no SCC occurred in prolonged tests (>900 hr) conducted under constant elongation conditions at stresses well above the yield strength. Localized corrosion, without signs of crack initiation, was observed both at the corrosion potential and at a slightly anodic potential.

No SCC occurred in the chloride concentration range extending from 1,000 to 10,000 ppm (Figure 3-2) under a wide range of experimental conditions, including the presence of crevice geometries. The results plotted in Figure 3-2 indicate that a decrease of the strain rate from 1.0×10^{-6} to 2.2×10^{-7} s^{-1} did not induce crack initiation under similar environmental conditions even in the presence of thiosulfate, which is one of the critical species that could be generated inside a crevice by the dissolution of sulfide inclusions. In this chloride concentration range, it was also difficult to avoid the occurrence of pitting as predominant phenomenon. Although the potentials selected were well below the extrapolation of the line representing the dependence of E_p with chloride concentration (Figure 3-2), pitting corrosion was observed in all these specimens as noted in Table 3-3.

It must be emphasized, however that Tamaki et al. (1990) were able to initiate cracks in type 316 SS in relatively dilute chloride solutions (180 to 18,000 ppm Cl^-) at 80 °C by using a tapered double-cantilever beam specimen with a sufficiently wide but narrow crevice. Transgranular cracks initiated and grew under applied potentials above E_{SCCEV} and stress intensities (K_I) greater than 4.0 MPa$\cdot m^{1/2}$. Transgranular cracking of solution-annealed type 316 SS has been observed in slow strain rate tests in the presence of very low (5 ppm) chloride concentrations as NaCl when smooth tensile specimens were tested (Yang et al., 1992) but at temperatures above 150 °C. In addition to the differences in specimen geometry, stressing techniques and other experimental conditions (e.g., temperature), it is entirely possible that the occurrence of SCC observed by Tamaki et al. (1990) and Yang et al. (1992) can be attributed, at least partially, to the higher carbon content of type 316 SS with respect to that of type 316L.

It appears that acidic, high-chloride concentrations are required locally to initiate cracks in type 316L SS at temperatures below 100 °C. In dilute solutions, a tight crevice is necessary to generate such acidic, localized environment sufficiently enriched in chloride ions in the presence of the required tensile stresses. Tsujikawa et al. (1994) used a spot-welded specimen, which had a tight metal/metal crevice and high residual stresses, to demonstrate that cracks are initiated in the creviced area at potentials just above E_{SCCEV} in a variety of Fe-18Cr-14Ni alloys, containing other alloying elements, in dilute NaCl solutions at 80 °C. At even higher potentials, crevice corrosion predominated. As summarized in Table 3-4, several tests conducted in 1 M NaCl solution using specimens with a specially designed crevice-forming device did not lead to the initiation of cracks, because pitting corrosion predominated in the crevice region. However, the initiation of minor cracks, without any noticeable growth, was noted in one of the galvanostatic tests. Presumably, tests conducted at a lower applied current may lead to crack growth without the competing effect of localized corrosion propagation.

Contrary to the results of slow strain rate tests in dilute chloride solutions, SCC was often observed in constant deflection tests, even in the absence of thiosulfate, as summarized in Table 3-7. The presence of thiosulfate, however, significantly enhanced SCC susceptibility. Cracks were mostly detected above the vapor/solution interface, indicating that the local environment created as a liquid film on the

specimen surface could be more detrimental than the bulk liquid environment. The existence of stagnant conditions, promoted by the elimination of a purging gas, appears to create a more severe environment than that arising from the continuous bubbling of synthetic air. This is apparently reflected in the higher potential obtained without gas purging (-130 mV_{SCE}) with respect to that (< -200 mV_{SCE}) measured in the presence of purged air. It is possible that H_2S, generated by reduction of thiosulfate at the metal surface, could be more easily oxidized by oxygen in a process assisted by the solution agitation promoted by gas bubbling and therefore eliminated from the solution as a cracking promoter. However, additional information is needed to confirm this interpretation.

No convincing explanation can be offered at the present time for the differences observed between the results of slow strain rate and constant deflection tests. Explanations based on differences in oxygen concentration, potential distributions at the vapor/solution interface, or exposure times are not considered to be satisfactory. Currently, the possibility of heat to heat variation for heats A and B is being investigated.

As noted in Figure 3-21, SCC in 1,000 ppm chloride solutions containing thiosulfate occurred at potentials below the E_{rp} line. The explanation for the occurrence of SCC at such low potentials is similar to that offered above for the slow strain rate tests conducted at higher chloride concentrations. However, the occurrence of pitting and even SCC in plain chloride solutions at potentials below that line is not explainable, but it may be attributed to the fact that the potential exhibited significant variations during these prolonged tests.

In more concentrated chloride solutions, SCC of type 316L SS was observed in constant deflection tests conducted in both LiCl and NaCl solutions at concentrations (5.8 molal) at which no cracking was detected in slow strain rate tests, as a comparison of the results shown in Tables 3-2 and 3-8 reveals. The addition of thiosulfate further increased the susceptibility to SCC in agreement with the result obtained in the slow strain rate tests included in Table 3-5.

4.2 STRESS CORROSION CRACKING OF ALLOY 825

The results shown in Table 3-6 and Figure 3-15 clearly indicate that mill-annealed alloy 825 only failed by SCC in slow strain rate tests when exposed to $MgCl_2$ solutions at a chloride concentration of 14.0 molal and a temperature of 120 °C. In contrast, SCC did not occur in LiCl solutions in which the chloride concentration was equal to 9.1 molal at 110 °C. These results indicate that under the experimental conditions used in these tests, particularly in terms of temperature and strain rate, SCC cannot be promoted regardless of the cation at chloride concentrations less than or equal to 9.1 molal, even at acidic pHs. Instead of SCC, the dominant failure mode was ductile failure, accompanied by pitting corrosion. Under equivalent testing conditions, mill-annealed type 316L SS was found to be susceptible to SCC at chloride concentrations greater than 7.2 molal. In 40-percent $MgCl_2$ solution at 120°C the elongation to failure for type 316L SS was found to be 7.4 percent at the open-circuit potential and 4.6 percent at a 20-mV anodic overpotential, whereas for alloy 825 the values were 44 and 36 percent, respectively.

The addition of thiosulfate to a 5.8 molal NaCl solution promoted transgranular SCC of type 316L SS. However, as shown in Table 3-5 and Figure 3-15, no SCC was observed on alloy 825 under the same testing condition or under more severe conditions prompted by the use of a notched specimen at a lower extension rate over a very extended period. Tsujikawa et al. (1993) reported that alloy 825 did

not exhibit SCC in 20-percent NaCl solution (4.3 molal) containing 0.001 to 0.1 M $Na_2S_2O_3$ (pH 4.0) at 80 °C by conducting slow strain rate tests and constant load tests at applied stresses above the yield strength of the alloy. As indicated in Figure 3-15, pitting was observed in the thiosulfate-containing solution. The open-circuit and the anodic potentials used for testing in this environment are well below the plotted values of E_{rp}. However, it should be noted that metastable sulfur oxyanions, such as $S_2O_3^{2-}$, induce a significant decrease in E_p and E_{rcrev} for type 304 SS when added to chloride-containing solutions with respect to the plain chloride environment (Newman et al., 1982; Nakayama et al., 1993). A similar effect can be expected for alloy 825, and this may explain the occurrence of pitting corrosion at such low potentials.

The constant deflection tests confirmed the results of the slow strain rate tests in the case of alloy 825 in the sense that no SCC was found within the same range of chloride concentrations using both test methods. SCC was observed only in 40-percent $MgCl_2$ solution at 120 °C using slow strain rate tests. U-bend tests are currently being conducted in the same solution to further compare both test methods. A large number of constant deflection tests was conducted for extended periods in concentrated chloride solutions close to the solubility of NaCl at 95 °C to confirm the superior resistance to SCC of alloy 825 compared to type 316L SS using a different test technique. As noted above, SCC of type 316L SS was observed in constant deflection tests in both LiCl and NaCl solutions at concentrations (5.8 molal) at which no cracking was detected in slow strain rate tests. This difference in behavior can be expected from their chemical compositions (Sridhar and Cragnolino, 1992). The higher nickel content of alloy 825 combined with the higher levels of chromium and molybdenum makes this alloy far more resistant to SCC in chloride-containing environments that any of the austenitic SS.

Contrary to the case of type 316L SS in which a significant susceptibility to SCC in constant deflection tests was detected in the vapor phase under conditions leading to the formation of liquid film on the surface, localized corrosion in the form of pitting was the dominant phenomenon in alloy 825. The SCC resistance of alloy 825 needs to be explored under a wide range of environmental conditions because the alloy exhibits a significant susceptibility to localized corrosion. Stress corrosion cracking can occur as a competitive phenomenon when the tendency to localized corrosion becomes marginal. The constant deflection tests were extended for several months to determine if cracks can be initiated from pits. Apparently this is not the case. It cannot be disregarded, however, that the initiation of cracks could be promoted through the alteration of the surface or near-surface conditions by the introduction of very localized plastic deformation via cold-work or microchemical modifications through surface depletion of some alloying element or thickening of the passive film by oxidation in air (Dunn et al., 1993a; 1993b). Sensitization to intergranular corrosion promoted by prolonged heat treatment at temperatures above 550 °C (Cragnolino and Sridhar, 1993) leading to carbide precipitation and presumably to chromium depletion at grain boundaries may have an important effect on SCC of alloy 825. Additional experiments are needed to investigate these effects. In particular, constant deflection tests, using double U-bend specimens in which the formation of a crevice environment in regions of highly localized tensile stress is promoted, are being conducted under a variety of controlled potential and surface conditions to attain a better understanding of the events that may lead to crack initiation.

5 SUMMARY AND RECOMMENDATIONS

The SCC of container materials proposed as components of the waste package is being examined in Task 2 of the IWPE project. In the context of the NRC role as a reviewer of the license application for construction of a HLW repository, the objective of this task is to assess test methodologies for evaluating the occurrence of SCC, and the applicability of appropriate parameters for long-term performance prediction. The experimental investigation to date has concentrated on two candidate Fe-Cr-Ni-Mo alloys, type 316L SS and alloy 825. The fundamental approach in the study of SCC has been the use of short-term test techniques to delineate the effects of various environmental factors and the use of the parameters derived from short-term tests for long-term prediction.

Slow strain rate tests and constant deflection tests on type 316L SS and alloy 825 are being used to define environmental conditions in terms of solution composition, pH, and temperature, as well as potential ranges that may promote SCC. The environments studied are chloride-containing solutions that simulate variations of groundwater environments produced by evaporation of water and concentration of salts. The ultimate goal is to determine if a critical potential for SCC exists, and to define the relationship between this potential and the repassivation potential for pitting/crevice corrosion. If such critical potential for SCC exists, it can be used as a bounding parameter for the prediction of long-term behavior, assuming that various combinations of tensile stress conditions in the container can promote cracking under the range of environments anticipated at the proposed repository site.

The results generated so far are consistent with the assumption that the repassivation potential for localized corrosion constitutes a lower bound for the critical potential for SCC in the case of type 316L SS. However, the range of chloride concentrations over which SCC occurred seems to be dependent on the test technique. In slow strain rate tests, SCC of type 316L SS was observed when exposed to $MgCl_2$ and LiCl solutions at chloride concentrations equal to or greater than 7.2 molal and temperatures above 100 °C. Although SCC occurred under open-circuit conditions, it was significantly enhanced at slightly anodic potentials. On the contrary, SCC did not occur in NaCl and LiCl solutions in which the chloride concentration was 6.2 molal at 95 °C. This is close to the maximum concentration attainable in NaCl due to solubility limitations. These results indicate that under the experimental conditions used in these tests, particularly in terms of temperature and strain rate, no SCC can be promoted regardless of the cation at chloride concentrations equal to or lower than 6.2 molal, even at acidic pHs. The addition of thiosulfate promoted SCC in solutions containing 5.8 mol Cl^-/kg water both at the open-circuit and anodic-applied potentials but not at lower chloride concentrations.

No SCC occurred in the chloride concentration range extending from 1,000 to 10,000 ppm at 95 °C, under a wide range of experimental conditions, including the presence of crevice geometries and the addition of thiosulfate, at potentials at which SCC should be expected. In this chloride concentration range, pitting occurred as the predominant phenomenon, although potentials were well below the line representing the dependence of E_p on chloride concentration. Incipient cracks were observed in a galvanostatic test under crevice conditions in 1 M NaCl solution ($\approx$35,450 ppm chloride). Although the failure was ductile and accompanied by pitting corrosion, this result suggests that SCC may be promoted in slow strain rate tests under crevice conditions at this chloride concentration over a very narrow range of potentials near E_{rp}.

Contrary to the results of slow strain rate tests, SCC of type 316L SS occurred in constant deflection tests in dilute chloride solutions (1,000 ppm) at 95 °C and potentials ranging from -130 to -240 mV_{SCE},

with and without the addition of thiosulfate. The presence of thiosulfate, however, significantly enhanced the SCC susceptibility. Cracks were detected mostly above the vapor/solution interface, indicating that the local environment created as a liquid film on the specimen surface could be more detrimental than the bulk liquid environment. In more concentrated chloride solutions, SCC was observed in constant deflection tests conducted in both LiCl and NaCl solutions at concentrations (5.8 molal) at which no cracking was detected in slow strain rate tests. The addition of thiosulfate further increased the susceptibility to SCC in agreement with the result obtained in the slow strain rate tests.

Alloy 825 only failed by SCC in slow strain rate tests when exposed to $MgCl_2$ solutions at a chloride concentration of 14.0 molal and a temperature of 120 °C. In contrast, SCC did not occur in LiCl and NaCl solutions in which the chloride concentration was equal to 9.3 molal or lower at temperatures below 110 °C. These results indicate that under the experimental conditions used in these tests, particularly in terms of temperature and strain rate, SCC cannot be promoted regardless of the cation at chloride concentrations less than or equal to 9.3 molal, even at acidic pHs. Instead of SCC, the dominant failure mode was ductile failure accompanied by pitting corrosion. SCC did not occur by the addition of thiosulfate to a chloride solution containing 5.8 mol Cl^-/kg water even under severe conditions prompted by the use of a notched specimen at a lower extension rate over a very extended period. The constant deflection tests confirmed the results of the slow strain rate tests in the case of alloy 825 in the sense that no SCC was found within the same range of chloride concentrations using both test methods. Contrary to the case of type 316L SS in which a significant susceptibility to SCC in constant deflection tests was detected in the vapor phase under conditions leading to the formation of liquid film on the surface, localized corrosion in the form of pitting, also near the vapor/solution interface, was the predominant phenomenon in alloy 825.

A wide range of chloride concentrations up to 6.2 molal is expected at temperatures around 100 °C under the environmental conditions anticipated to prevail at the proposed repository site, according to model calculations performed at the CNWRA (Walton, 1993; Cragnolino et al., 1993). Testing conducted at greater chloride concentrations, such as those obtained with $MgCl_2$ and LiCl, was used to demonstrate the concept of a critical potential for SCC at chloride concentration ranges within which SCC can be promoted in reasonable test times.

The approach adopted in this study considering the repassivation potential for localized corrosion as the critical potential for the occurrence of SCC needs further confirmation through additional testing. Based on the results and analyses of tests described in this report, the following activities are recommended:

- Perform experiments at various chloride concentrations in which cracks, once initiated at potentials higher than the critical potential for SCC, are arrested by decreasing the potential below that value.

- Perform a set of tests using fracture mechanics specimens to evaluate the effect of stress intensity on crack growth rate and determine the value of K_{Iscc}. These tests should cover a range of environmental conditions, in terms of chloride concentration, temperature, presence of thiosulfate and potential, using modified wedge-opening loading specimens to confirm the results of slow strain rate tests and constant deflection tests.

- Perform long-term experiments under constant deflection conditions, lasting from a few months to 5 yr at various chloride concentrations using potentials above and below the

critical potential for SCC to confirm the validity of this approach for performance evaluation. In the case of alloy 825, cold-worked specimens and specimens heat treated in the temperature range corresponding to sensitization should be included. These experiments should be performed in parallel with others conducted under open-circuit conditions in oxidizing environments. Eventually, the SCC of welded components, including weld-metal and heat-affected zones, should be investigated once the design of the waste package is more advanced.

- Conduct an integrated SCC/localized corrosion test in which heat transfer effects and the influence of periodic wet-dry cycles is investigated. Heat transfer conditions and wet-dry cycles can promote concentration of salts from a relatively dilute environment and, therefore, generate SCC susceptibility from an initially innocuous environment through the initiation, without significant propagation, of localized corrosion. This type of evolving environment is relevant to the proposed repository located in the unsaturated zone because following the temperature decay at the waste package surface and the surrounding rock, the stabilization of concentrated solutions is expected on the waste package surfaces.

In addition to type 316L SS and alloy 825, SCC studies should be extended to the materials considered for the outer disposal overpack of the current DOE design for the waste package. Materials such as wrought-ferritic steels, low-alloy steels, cast-ferritic steels, and ductile iron may be susceptible to SCC in the presence of bicarbonate solutions, as in the case of pipeline steels. The possible beneficial effect of galvanic coupling of these steels on the SCC of alloys, such as type 316L SS and alloy 825, should be investigated. The possibility of hydrogen embrittlement, as a result of such cathodic protection, should also be examined, particularly for alloy 825.

Part of this recommended work can be accomplished during the last phase of the current IWPE project, but most of the extended testing necessarily will be deferred to future projects. This is particularly true for integrated tests requiring adequate consideration of heat transfer conditions, fluid-flow regime, and wet-dry cycles, in addition to mechanical and electrochemical factors. Extension of the SCC studies to steels proposed for the outer disposal overpack also should be included in future projects.

6 REFERENCES

Abraham, T., H. Jain, and P. Soo. 1986. *Stress Corrosion Cracking Tests on High-Level Waste Container Materials in Simulated Tuff Repository*. NUREG/CR-4619. Washington, DC: Nuclear Regulatory Commission.

Alkire, R.C., and S.E. Lott. 1989. The role of inclusions of initiation of crevice corrosion of stainless steel. II. Theoretical studies. *Journal of the Electrochemical Society* 136: 3,256–3,262.

American Society for Testing and Materials. 1991. Standard practice for making and using U-bend stress-corrosion test specimens. *Annual Book of Standards*. Philadelphia, PA: American Society for Testing and Materials: 03.02: 96–101.

Beavers, J.A., and G.H. Koch. 1992. Limitations of the slow strain rate test for stress corrosion cracking testing. *Corrosion* 48: 256–264.

Beavers, J.A., N.G. Thompson, and C.L. Durr. 1992. *Pitting, Galvanic, and Long-Term Corrosion Studies on Candidate Container Alloys for the Tuff Repository*. NUREG/CR-5709. Columbus, OH: Cortest Columbus Technologies, Inc.

Buschek, T.A., D.G. Wilder, and J.J. Nitao. 1993. Large-scale *in situ* heater tests for hydrothermal characterization at Yucca Mountain. *Proceedings of the Fourth Annual International High Level Radioactive Waste Management Conference*. La Grange Park, IL: American Nuclear Society: 1854–1872.

Cragnolino, G.A., and N. Sridhar. 1992. *A Review of Stress Corrosion Cracking of High-Level Nuclear Waste Container Materials—I*. CNWRA 92-021. San Antonio, TX: Center for Nuclear Waste Regulatory Analyses.

Cragnolino, G.A., and N. Sridhar. 1993. *Long-Term Stability of High-Level Nuclear Waste Container Materials: I—Thermal Stability of Alloy 825*. CNWRA 93-003. San Antonio, TX: Center for Nuclear Waste Regulatory Analyses.

Cragnolino, G.A., N. Sridhar, J. Walton, R. Janetzke, T. Torng, J. Wu, and P. Nair. 1994. *"Substantially Complete Containment"—Example Analyses of a Reference Container*. CNWRA 94-003. San Antonio, TX: Center for Nuclear Waste Regulatory Analyses.

Duffo, G.S., I.A. Maier, and J.R. Galvele. 1988. The influence of temperature on the susceptibility of type 304 stainless steel to intergranular and transgranular stress corrosion cracking in LiCl solutions. *Corrosion Science* 28: 1,003–1,018.

Dunn, D.S., N. Sridhar, G.A. Cragnolino. 1993a. The effect of surface conditions on the localized corrosion of a candidate high-level waste container material. *Proceedings of the 12th International Corrosion Congress on Corrosion Control for Low-Cost Reliability*. Houston, TX: NACE International: 4,021–4,028.

Dunn, D.S., N. Sridhar, and G.A. Cragnolino. 1993b. Effects of surface conditions on the localized corrosion of alloy 825 high-level waste container material. Paper No. 94-138. *Corrosion/94.* Houston, TX: NACE International.

Farmer, J.C., G.E. Gdowski, R.D. McCright, and H.S. Ahluwalia. 1991. Corrosion models for performance assessment of high-level radioactive waste containers. *Nuclear Engineering and Design* 129: 57–88.

Geesey, G. 1993. *A Review of the Potential for Microbially Influenced Corrosion of High-Level Nuclear Waste Containers.* G.A. Cragnolino, ed. CNWRA 93-014. San Antonio, TX: Center for Nuclear Waste Regulatory Analyses.

International Organization for Standardization. 1989. *Corrosion of Metals and Alloys—Stress Corrosion Testing. Part 7: Slow Strain Rate Testing.* ISO 7539-7: 1989 (E). Geneva, Switzerland: International Organization for Standardization.

Linke, W.F. 1965. *Solubilities: Inorganic and Metal Organic Compounds.* Washington, DC: American Chemical Society: 959.

Lott, S.E., and R.C. Alkire. 1989. The role of inclusions on initiation of crevice corrosion of stainless steel. I. Experimental studies. *Journal of The Electrochemical Society* 136: 973–979.

Macdonald, D.D., and M. Urquidi-Macdonald. 1990. Thin-layer mixed-potential model for corrosion of high-level nuclear waste canisters. *Corrosion* 46: 380–390.

Manfredi, C., I.A. Maier, and J.R. Galvele. 1987. The susceptibility of AISI type 304 stainless steel to transgranular and intergranular SCC in 40% $MgCl_2$ solution at 100 °C. *Corrosion Science* 27: 887–903.

Murphy, W.M., and R.T. Pabalan. 1994. *Geochemical Investigations Related to the Yucca Mountain Environment and Potential Nuclear Waste Repository.* CNWRA 94-006. San Antonio, TX: Center for Nuclear Waste Regulatory Analyses.

Nakayama, G., H. Wakamatsu, and M. Akashi. 1993. Effects of chloride, bromide, and thiosulfate ions on the critical conditions for crevice corrosion of several stainless alloys as a material for geological disposal packages for nuclear waste. *Scientific Basis for Nuclear Waste Management XVI.* C.G. Interrante and R.T. Pabalan, eds. Pittsburgh, PA: Materials Research Society: 294: 323–328.

Newman, R.C., H.S. Isaacs, and B. Alman. 1982. Effects of sulfur compounds on the pitting behavior of type 304 stainless steel in near-neutral chloride solutions. *Corrosion* 38: 261–265.

Nuclear Regulatory Commission. 1992. *Draft License Application Review Plan for the Review of a License Application for a Geologic Repository for Spent Nuclear Fuel and High-Level Radioactive Waste Yucca Mountain, Nevada.* NUREG-1323. Washington, DC: Office of Nuclear Material Safety and Safeguards, Nuclear Regulatory Commission.

Okada, H., Y. Hosio, and S. Abe. 1971. Scanning electron microscopic observations of fracture surfaces of austenitic stainless steels in stress corrosion cracking. *Corrosion* 27: 424–428.

Patrick, W.C. 1986. *Spent Fuel Test—Climax: An Evaluation of the Technical Feasibility of Geologic Storage of Spent Nuclear Fuel in Granite—Final Report*. UCRL-53702. Livermore, CA: Lawrence Livermore National Laboratory.

Ramirez, A.L., ed. 1991. *Prototype Engineered Barrier System Field Test (PEBSFT) Final Report* UCRL-ID-106159. Livermore, CA: Lawrence Livermore National Laboratory.

Ruffner, D.J., G.L. Johnson, E.A. Platt, J.A. Blink, and T.W. Doering. 1993. Drift emplaced waste package thermal response. *Proceedings of the Fourth Annual International High Level Radioactive Waste Management Conference*. La Grange Park, IL: American Nuclear Society: 538–543.

Scully, J.C. 1971. Fractographic aspects of stress corrosion cracking. *Theory of Stress Corrosion Cracking in Alloys*. J.C. Scully, ed. Brussels, Belgium: North Atlantic Treaty Organization: 127–166.

Silcock, J.M., and P.R. Swann. 1979. Nucleation and growth of transgranular stress corrosion cracks in austenitic stainless steels. *Environment-Sensitive Fracture of Engineering Materials*. Z.A. Foroulis, ed. Warrendale, PA: The Metallurgical Society of AIME: 133–152.

Sridhar, N., and G.A. Cragnolino. 1992. Stress corrosion cracking of nickel-base alloys. *Stress Corrosion Cracking. Materials Performance and Evaluation*. R.H. Jones, ed. Materials Park, OH: ASM International: 131–179.

Sridhar, N., and G.A. Cragnolino. 1993. Applicability of repassivation potential for long-term prediction of localized corrosion of alloy 825 and type 316L stainless steel. *Corrosion* 49: 885–894.

Sridhar, N., G.A. Cragnolino, and D. Dunn. 1993a. *Experimental Investigations of Localized Corrosion of High-Level Waste Container Materials*. CNWRA 93-004. San Antonio, TX: Center for Nuclear Waste Regulatory Analyses.

Sridhar, N., J.C. Walton, G.A. Cragnolino, and P.K. Nair. 1993b. *Engineered Barrier System Performance Assessment Codes (EBSPAC) Progress Report—October 1, 1992, through September 25, 1993*. CNWRA 93-021. San Antonio, TX: Center for Nuclear Waste Regulatory Analyses.

Sridhar, N., G.A. Cragnolino, D.S. Dunn, and H.K. Manaktala. 1994. *Review of Degradation Modes of Alternate Container Designs and Materials*. CNWRA 94-010. San Antonio, TX: Center for Nuclear Waste Regulatory Analyses.

Stalder, F., and D.J. Duquette. 1977. Slow strain rate stress corrosion cracking of type 304 stainless steels. *Corrosion* 33: 67–72.

Szklarska-Smialowska, Z. 1986. *Pitting Corrosion of Metals*. Houston, TX: National Association of Corrosion Engineers: 201–236.

Takano, M. 1974. Effect of strain rate on stress corrosion cracking of austenitic stainless steel in $MgCl_2$ solutions. *Corrosion* 30: 441–446.

Tamaki, K., S. Tsujikawa, and Y. Hisamatsu. 1990. Development of a new test method for chloride stress corrosion cracking of stainless steel in dilute NaCl solutions. *Advances in Localized Corrosion*. H.S. Isaacs, U. Bertocci. J. Kruger, and S. Smialowska, eds. Houston, TX: National Association of Corrosion Engineers: 207–214.

Tsujikawa, S., Y. Soné, and Y. Hisamatsu. 1987. Analysis of mass transfer in a crevice region for a concept of the repassivation potential as a crevice corrosion characteristic. *Corrosion Chemistry within Pits, Crevices, and Cracks*. A. Turnbull, ed. London, U.K.: Her Majesty's Stationary Office: 171–186.

Tsujikawa, S., T. Shinohara, and W. Lichang. 1994. Spot-welded specimen potentiostatically kept just above the crevice repassivation potential to evaluate stress corrosion cracking susceptibility of improved type 304 stainless steels in NaCl solutions. *Applications of Accelerated Corrosion Tests to Service Life Prediction of Materials*. G. Cragnolino and N. Sridhar, eds. ASTM STP 1194. Philadelphia, PA: American Society for Testing and Materials: 340–354.

Tsujikawa, S., A. Miyasaka, M. Uedo, S. Ando, T. Shibata, T. Haruna, M. Katahira, Y. Yamane, T. Aoki, and T. Yamada. 1993. Alternative for evaluating sour gas resistance of low-alloy steels and corrosion-resistant alloys. *Corrosion* 49: 409–419.

U.S. Department of Energy. 1988. *Site Characterization Plan for the Yucca Mountain Site, Nevada Research and Development Area, Nevada*. DOE/RW-0199. Washington, DC: U.S. Department of Energy.

U.S. Department of Energy. 1993a. *MPC Implementation Program Conceptual Design Phase. Volume I—MPC Conceptual Design Summary Report*. DOC ID: A2000000-00811-5705-00001. WBS: 3.1.07. Washington, DC: U.S. Department of Energy, Office of Civilian Radioactive Waste Management.

U.S. Department of Energy. 1993b. *A Preliminary Evaluation of Using Multi-Purpose Canisters Within the Civilian Radioactive Waste Management System. Revision 0*. CRWMS M&O Document No. A00000000-AA-07-00002. Vienna, VA: TRW Environmental Safety Systems, Inc.

Walton, J.C. 1993. Effects of evaporation and solute concentration on presence and composition of water in and around the waste package at Yucca Mountain. *Waste Management* 13: 293–301.

Yang, W., J. Conglenton, O. Kohneh-Chari, and P. Sajdl. 1992. The strain for stress corrosion cracking initiation in type 316 stainless steel in high temperature water. *Corrosion Science* 33: 735–750.

Zimmerman, R.M., R.L. Schuch, D.S. Mason, M.L. Wilson, M.E. Hall, M.P. Board, R.P. Bellman, and M.P. Blanford. 1986. *Final Report: G-Tunnel Heated Block Experiment*. SAND84-2620. Albuquerque, NM: Sandia National Laboratories.